

ASARCO STABLE NIGHTTIME
CONDITION FLUID MODELING INVESTIGATION

by

R. L. Petersen,* J. E. Cermak**
and M. Hisato***

prepared for

North American Weather Consultants
600 Norman Firestone Road
Goleta, California 93017

Fluid Dynamics and Wind Engineering Program
Department of Civil Engineering
Colorado State University
Fort Collins, Colorado 80523

May 14, 1980

Engineering Services

NOV 4 1980

Branch Library

CER79-80RLP-JEC-MH58

*Research Assistant Professor
**Director, Fluid Dynamics and Diffusion Laboratory
***Graduate Research Assistant



U18401 0075536

ABSTRACT

A physical modeling study was conducted in the Colorado State University meteorological wind tunnel of the dispersion of plumes emitted from ASARCO and Kennecott stacks near Hayden, Arizona. Ground-level concentration measurements were obtained in the vicinity of the Montgomery Ranch Monitoring station to determine percent contribution due to each source -- ASARCO and Kennecott.

The results of the study showed that the Kennecott short stack contributed 19 percent of the ground-level concentration at the Montgomery Ranch station for the condition simulated. The contribution to total emissions for this stack was 2 percent. The ASARCO stack contributed 29 percent of the ground-level concentration while contributing 80 percent of the total emissions.

TABLE OF CONTENTS

<u>Chapter</u>	<u>Page</u>
ABSTRACT	i
LIST OF FIGURES	iii
LIST OF TABLES	v
LIST OF SYMBOLS	vi
1 INTRODUCTION	1
2 SUMMARY	2
3 WIND-TUNNEL SIMILARITY REQUIREMENTS	3
3.1 Basic Equations	3
3.2 Non-Equal Scaling Parameters	4
3.3 Equal Scaling Parameters	9
4 EXPERIMENTAL METHOD	12
4.1 Summary	12
4.2 Scale Model and Wind Tunnel	13
4.3 Flow Visualization	14
4.4 Gas Tracer Technique	14
Averaging Time	18
4.5 Velocity and Temperature Measurements	18
5 RESULTS	21
5.1 Velocity and Temperature Measurements	21
5.2 Plume Transport and Diffusion Results	22
Photographic Results	22
Concentration Measurement Results	24
REFERENCES	26
FIGURES	28
TABLES	46
APPENDIX A	61
Project Correspondence	61

LIST OF FIGURES

<u>Figure</u>		<u>Page</u>
3-1	Drawing of Model Stack used for ASARCO Stable Wind Tunnel Tests.	29
4-1	Meteorological Wind Tunnel. Fluid Dynamics and Diffusion Laboratory. Colorado State University.. . . .	30
4-2	Topographic Map of the Area Modeled in the Wind Tunnel showing the Velocity and Temperature Profile Measurement Locations and the Stack Locations	31
4-3	Photographs showing a) the Terrain in the Tunnel looking into the Flow and b) the Approach to the Model Terrain and the Upwind Cooling Plates	32
4-4	Map showing Ground-Level Concentration Sampling Locations and Location Number	33
4-5	Photographs of a) the Tracer Gas Sampling System and b) the Hewlett Packard Gas Chromatograph and Integrator	34
5-1	Dimensionless Velocity and Temperature Profile at Location No. 1 for $T_O = 6.5^{\circ}\text{C}$, $T_{\infty} = 57.2^{\circ}\text{C}$ and $u_m = 0.964 \text{ m/sec}$ 	35
5-2	Dimensionless Velocity and Temperature Profile at Location No. 2 for $T_O = 10.5^{\circ}\text{C}$, $T_{\infty} = 60.1^{\circ}\text{C}$ and $u_m = 0.886 \text{ m/sec}$ 	36
5-3	Dimensionless Velocity and Temperature Profile at Location No. 3 for $T_O = 11.5^{\circ}\text{C}$, $T_{\infty} = 59.0^{\circ}\text{C}$ and $u_m = 0.972 \text{ m/sec}$ 	37
5-4	Dimensionless Velocity and Temperature Profile at Location No. 4 for $T_O = 9.1^{\circ}\text{C}$, $T_{\infty} = 57.4^{\circ}\text{C}$ and $u_m = 1.106 \text{ m/sec}$ 	38
5-5	Dimensionless Velocity and Temperature Profile at Location No. 5 for $T_O = 8.2^{\circ}\text{C}$, $T_{\infty} = 56.7^{\circ}\text{C}$ and $u_m = 1.087 \text{ m/sec}$ 	39
5-6	Dimensionless Velocity and Temperature Profile at Location No. 6 for $T_O = 4.5^{\circ}\text{C}$, $T_{\infty} = 56.1^{\circ}\text{C}$ and $u_m = 1.078 \text{ m/sec}$ 	40
5-7	Dimensionless Velocity and Temperature Profile at Location No. 7 for $T_O = 6.1^{\circ}\text{C}$, $T_{\infty} = 56.8^{\circ}\text{C}$ and $u_m = 0.935 \text{ m/sec}$ 	41

<u>Figure</u>		<u>Page</u>
5-8	Photograph of Plume Transport from a) ASARCO Tall Stack and b) Kennecott Tall Stack under Stable Stratification for a Southeast Wind	42
5-9	Results of Concentration Measurements for ASARCO Tall Stack	43
5-10	Results of Concentration Measurements for Kennecott Tall Stack (Kennecott #1)	44
5-11	Results of Concentration Measurements for Kennecott Short Stack (Kennecott #2).	45

LIST OF TABLES

<u>Table</u>		<u>Page</u>
3.1	Model and Prototype Parameters for the ASARCO- Stable Evaluation	47
5.1	Velocity and Temperature Profile at Location 1	48
5.2	Velocity and Temperature Profile at Location 2	49
5.3	Velocity and Temperature Profile at Location 3	50
5.4	Velocity and Temperature Profile at Location 4	51
5.5	Velocity and Temperature Profile at Location 5	52
5.6	Velocity and Temperature Profile at Location 6	53
5.7	Velocity and Temperature Profile at Location 7	54
5.8	Example of Power Law Exponent Variations with Stability from a) Touma, 1977 and b) Sutton, 1953	55
5.9	Summary of Velocity Profile Characteristics	56
5.10	Concentration Results for ASARCO Tall Stack	57
5.11	Concentration Results for Kennecott Stack #1	58
5.12	Concentration Results for Kennecott Stack #2	59
5.13	Summary of Stable Wind Tunnel Tests for ASARCO	60

LIST OF SYMBOLS

<u>Symbol</u>		<u>Units</u>
B_o	Buoyancy ratio $\left[\frac{R^3}{Fr^2} \frac{D}{H} \right]$	(-)
C_p	Specific heat at constant pressure	$(m^2 s^{-2} K^{-1})$
D	Stack inside diameter	(m)
E	Hot-wire voltage	(V)
E_c	Eckert number $\left[u_o^2 / (C_{p_o} \Delta T_o) \right]$	(-)
F_L	Lagrangian spectral function	(s)
Fr_{Γ}	Stack Froude number $\left[\frac{u_s}{\sqrt{g\Gamma d}} \right]$	(-)
Fr	Modified stack Froude number $\left[\frac{u_s}{\sqrt{g\gamma D}} \right]$	(-)
g	Acceleration due to gravity	(ms^{-2})
H_s	Height of stack	(m)
$i_{x,y,z}$	Turbulence intensity in x, y or z direction	(l)
I	Current through wire	(a)
k	Thermal conductivity	$(Wm^{-1}K^{-1})$
K	Dimensionless concentration $\left[\frac{\chi u_{\infty} \delta^2}{\chi_o V} \right]$	(-)
L	Length scale or Monin Obukhov length scale	(m)
M_o	Momentum ratio $\left[(1-\gamma) R^2 D^2 / H_s^2 \right]$	(-)
n	Frequency, power law exponent or King's law exponent	(varies)
Pr	Prandtl number $\left[\frac{v_o \rho_o C_{p_o}}{k_o} \right]$	(-)
R	Velocity ratio (u_s / u_a)	(-)

<u>Symbol</u>		<u>Units</u>
Re	Reynolds number $\left[\frac{L_o u_o}{\nu_o} \right]$	(-)
Ri	Richardson number $\frac{g}{T} \left[\frac{\frac{\partial \theta}{\partial z}}{\frac{\partial u^2}{\partial z}} \right]$	(-)
Ro	Rossby number $\left[\frac{L_o \Omega_o}{u_o} \right]$	(-)
R(τ)	Autocorrelation	(-)
t, τ , ξ	Time or time scale	(s)
T, θ	Temperature or potential temperature	(K)
t ₁	Center of gravity of autocorrelation curve	(s)
t _o	Integral time scale	(s)
u	Ambient velocity	(m/s)
u _a	Ambient velocity at reference height	(m/s)
u _m	Maximum ambient velocity	(m/s)
u _s	Stack exit velocity	(m/s)
u _∞	Velocity at free stream (600 m full-scale)	(m/s)
u _*	Friction velocity	(m/s)
V	Volume flow	(m ³ s ⁻¹)
w'	Deviation from mean vertical velocity	(m/s)
x, y, z	Cartesian coordinates	(-)
z	Height above ground	(m)

Greek Symbols

<u>Symbol</u>	<u>Definition</u>	<u>Units</u>
χ	Concentration	(ppm)
χ_0	Source strength	(ppm)
δ	Reference height (600 m full-scale)	(m)
Γ	Density ratio $\left[\frac{\rho_a - \rho_s}{\rho_s} \right]$	(-)
γ	Modified density ratio $\left[\frac{\rho_a - \rho_s}{\rho_a} \right]$	(-)
Λ	Length scale	(m)
ν	Kinematic viscosity	($m^2 s^{-1}$)
Ω	Angular velocity	(s^{-1})
ϕ^*	Dissipation term	(-)
ρ	Density	(gm^{-3})
σ_z, σ_y	Vertical and horizontal standard deviation of concentration distribution	(m)

Subscripts

<u>Symbol</u>	<u>Definition</u>
a	Pertaining to ambient conditions
i,j,k	Tensor summation indices
m	Model
o	General reference quantity or initial condition
p	Prototype
s	Pertaining to stack exit conditions
∞	Free stream

Superscripts

'	Root-mean-square of quantity
*	Dimensionless parameter

ASARCO Stable Nighttime Condition
Fluid Modeling Investigation

by

R. L. Petersen, J. E. Cermak and M. Hisato

1. INTRODUCTION

The purpose of this study is to determine the ground-level SO₂ concentrations due to the ASARCO 304.9 m stack and the Kennecott 182.9 and 24.4 m stacks under stable southeast flow. These stacks are situated near Hayden, Arizona. Specifically, ASARCO is interested in the expected SO₂ concentrations at the Montgomery Ranch field monitoring station due to each source. The conditions to be modeled were specified in a letter dated September 26, 1979 from L. G. Cahill, ASARCO to G. H. Taylor, North American Weather Consultants. G. H. Taylor subsequently authorized Colorado State University to begin work on the project in a December 10, 1979 letter to R. L. Petersen. This correspondence is included in Appendix A.

To meet the project objectives a physical modeling study was conducted in the Colorado State University meteorological wind tunnel. A 1 to 3072 scale model of the terrain for a southeast wind direction along with scale models of the stacks was constructed and positioned in the wind tunnel. A stable boundary layer was then generated and measurements of ground-level concentration were obtained at 24 locations. Several of the locations were near the Montgomery Ranch field monitoring station. The results of the measurements were then analyzed and the ground-level SO₂ concentration due to each source determined.

Included in this report are a summary, the similarity criteria for physical modeling, a description of the experimental methods and the results. Color slides, black and white photographs and a motion picture supplement this report.

2. SUMMARY

A physical modeling study of the transport and diffusion of plumes emitted from the ASARCO 304.9 m and Kennecott 182.9 and 24.4 m stacks was conducted under a simulated stable southeast flow condition. Ground-level concentration measurements were obtained in the vicinity of the Montgomery Ranch monitoring station to determine the percent of the total measured SO_2 due to each source.

The results of the wind tunnel simulation showed that the ASARCO 304.9 m, Kennecott 182.9 m and Kennecott 24.4 m stacks contributed 29, 52 and 19 percent respectively of the total measured SO_2 at the Montgomery Ranch station. The respective percent of total emissions were 80, 18 and 2 percent. Hence a source only emitting 2 percent of the total emissions contributes 19% of the total ground-level SO_2 concentration.

In conclusion the study demonstrates that stack height and emission rate should be considered simultaneously when planning strategies for attainment or maintenance of ambient air quality standards.

3. WIND-TUNNEL SIMILARITY REQUIREMENTS

3.1 Basic Equations

The basic equations governing atmospheric and plume motion (conversion of mass, momentum and energy) may be expressed in the following dimensionless form (Cermak, 1974):

$$\frac{\partial \rho^*}{\partial t^*} + \frac{\partial (\rho^* u_i^*)}{\partial x_i^*} = 0, \quad (3.1)$$

$$\left. \begin{aligned} \frac{\partial u_i^*}{\partial t^*} + u_j^* \frac{\partial u_i^*}{\partial x_j^*} - \left[\frac{L_o \Omega_o}{u_o} \right] 2\epsilon_{ijk} \Omega_j^* u_k^* = \\ - \frac{\partial p^*}{\partial x_i^*} - \left[\frac{\Delta T_o L_o g_o}{T_o u_o^2} \right] \Delta T^* g^* \delta_{i3} \\ + \left[\frac{v_o}{u_o L_o} \right] \frac{\partial^2 u_i^*}{\partial x_k^* \partial x_k^*} + \frac{\partial}{\partial x_j^*} (-\overline{u_i^* u_j^*}) \end{aligned} \right\} \quad (3.2)$$

and

$$\left. \begin{aligned} \frac{\partial T^*}{\partial t^*} + u_i^* \frac{\partial T^*}{\partial x_i^*} = \left[\frac{k_o}{\rho_o C_{p_o} v_o} \right] \left[\frac{v_o}{L_o u_o} \right] \frac{\partial^2 T^*}{\partial x_k^* \partial x_k^*} \\ + \frac{\partial}{\partial x_i^*} (-\overline{\theta^* u_i^*}) + \left[\frac{v_o}{u_o L_o} \right] \left[\frac{u_o^2}{C_{p_o} (\Delta T)_o} \right] \phi^* \end{aligned} \right\} \quad (3.3)$$

The dependent and independent variables have been made dimensionless (indicated by an asterisk) by choosing appropriate reference values.

For exact similarity, the bracketed quantities and boundary conditions must be the same in the wind tunnel and in the plume as they are in the corresponding full-scale case. The complete set of requirements for similarity is:

- 1) Undistorted geometry
- 2) Equal Rossby number: $Ro = u_o / (L_o \Omega_o)$

- 3) Equal gross Richardson number: $Ri = \frac{\Delta T_o g_o L_o}{T_o u_o^2}$
- 4) Equal Reynolds numbers: $Re = u_o L_o / \nu_o$
- 5) Equal Prandtl number: $Pr = (\nu_o \rho_o C_{p_o}) / k_o$
- 6) Equal Eckert number: $Ec = u_o^2 / [C_{p_o} (\Delta T)_o]$
- 7) Similar surface-boundary conditions
- 8) Similar approach-flow characteristics.

For exact similarity, each of the above parameters must be matched in model and prototype for the stack gas flow and ambient flow separately. Naturally, the reference quantities will change depending on which flow is being considered. To insure that the stack gas rise and dispersion are similar relative to the air motion, three additional similar parameters are required (Snyder, 1979; Petersen et al., 1977):

- 9) Velocity ratio: $R = \frac{u_s}{u_a}$
- 10) Froude number: $Fr_\Gamma = \frac{u_s}{\sqrt{g\Gamma D}}$
- 11) Density ratio: $\Gamma = \frac{\rho_a - \rho_s}{\rho_s}$

All of the above requirements cannot be simultaneously satisfied in the model and prototype. However, some of the quantities are not important for the simulation of many flow conditions. The parameters which are equated and those which are not in model and prototype will be discussed in the following subsections.

3.2 Non-Equal Scaling Parameters

For this study equal Reynolds number for model and prototype is not possible since the length scaling is 1:3072 and unreasonably high

model velocities would result. However, this inequality is not a serious limitation.

The Reynolds number related to the stack exit is defined by

$$Re_s = \frac{u_s D}{\nu_s} .$$

The plume rise will become independent of Reynolds number if the plume becomes fully turbulent at the stack exit. Hoult and Weil (1972) reported that plumes appear to be fully turbulent for exit Reynolds numbers greater than 300. Their experimental data show that the plume trajectories are similar for Reynolds numbers above this critical value. In fact the trajectories appear similar down to $Re_s = 28$ if only the buoyancy dominated portion of the plume trajectory is considered. Hoult and Weil's study was in a laminar cross flow (water tank) with low ambient turbulence levels, and hence the rise and dispersion of the plume would be predominantly dominated by the plume's own self-generated turbulence. For this study, u_s and D vary over a range to give Re_s of 59, 107 and 250 for Kennecott stack #2, Kennecott stack #1 and the ASARCO tall stack, respectively. As is evident stack Reynolds numbers below 300 were required for the study. From the work of Hewett et al. (1971) it was found that fully turbulent plumes could be obtained for stack Reynolds numbers of 150 provided that the flow was tripped at the stack. All stacks were designed with such a trip as is shown in Figure 3-1. The only plume which did not appear turbulent was the Kennecott small stack. The result of a non-turbulent plume is a larger initial plume rise and smaller ground-level concentrations which gives a conservative result for this study.

For similarity in the region dominated by ambient turbulence consider Taylor's (1921) relation for diffusion in a stationary homogeneous turbulence

$$\sigma_z^2(t) = \overline{w'^2} \int_0^t \int_0^t R(\xi) d\xi dt \quad (3.4)$$

which can be simplified to (see Csanady, 1973):

$$\sigma_z^2(t) \cong \overline{w'^2} t^2 \cong i_z^2 x^2 \quad (3.5)$$

for short travel times; or,

$$\sigma_z^2(t) = \overline{w'^2} t_o(t-t_1); \quad (3.6)$$

for long travel times where:

$$t_o = \int_0^\infty R(\tau) d\tau \quad (3.7)$$

is an integral time scale, and:

$$t_1 = \frac{1}{t_o} \int_0^\infty \tau R(\tau) d\tau \quad (3.8)$$

is the center of gravity of the autocorrelations curve. Hence, for geometric similarity at short travel times,

$$\frac{[\sigma_z^2]_m}{[\sigma_z^2]_p} = \frac{[L^2]_m}{[L^2]_p} = \frac{[i_z^2 x^2]_m}{[i_z^2 x^2]_p}$$

or,

$$[i_z]_m = [i_z]_p. \quad (3.9)$$

For similarity at long travel times

$$\begin{aligned} \frac{L_m^2}{L_p^2} &= \frac{[\sigma_z^2]_m}{[\sigma_z^2]_p} = \frac{[\overline{w'^2} t_o(t-t_1)]_m}{[\overline{w'^2} t_o(t-t_1)]_p} \\ &= \frac{[i_z^2]_m}{[i_z^2]_p} \frac{[t_o(t-t_1) \cdot u^2]_m}{[t_o(t-t_1) \cdot u^2]_p} = \frac{[Li_z^2 \Lambda]_m}{[Li_z^2 \Lambda]_p}, \end{aligned}$$

if it is assumed $t_1 \ll t$, $t_o \cdot u = \Lambda$ and $t \cdot u = L$. Thus, the turbulence

length scales must scale as the ratio of the model to prototype length scaling if $(i_z)_m = (i_z)_p$ or,

$$\frac{L_m}{L_p} = \frac{\Lambda_m}{\Lambda_p} \quad (3.10)$$

An alternate way of evaluating the similarity requirement is by putting 3.4 in spectral form or (Snyder, 1972);

$$\begin{aligned} \sigma_z^2 &= \overline{w'^2 t^2} \int_0^\infty F_L(n) \left[\frac{\sin \pi n t}{\pi n t} \right]^2 dn \\ &= \overline{w'^2 t^2} I \end{aligned} \quad (3.11)$$

where

$$I = \int_0^\infty F_L(n) \left[\frac{\sin \pi n t}{\pi n t} \right]^2 dn$$

F_L = Langrangian Spectral function.

The quantity in brackets is a filter function the form of which can be seen in Pasquill (1974). In brief for $n > 1/t$ the filter function is very small and for $n < 1/10t$ virtually unity.

For geometric similarity of the plume the following must be true:

$$\frac{L_m^2}{L_p^2} = \frac{[\sigma_z^2]_m}{[\sigma_z^2]_p} = \frac{[\overline{w'^2 t^2 I}]_m}{[\overline{w'^2 t^2 I}]_p} = \frac{[L^2 i_z^2 I]_m}{[L^2 i_z^2 I]_p}$$

or,

$$\frac{[i_z^2 I]_m}{[i_z^2 I]_p} = 1 \quad (3.12)$$

If $[i_z]_m = [i_z]_p$ the requirement is $I_m = I_p$. For short travel times, the filter function is essentially equal to one; hence, $I_m = I_p = 1$ and the same similarity requirement as previously deduced for short travel times is obtained (Equation 3.9).

For long travel times the larger scales (smaller frequencies) of turbulence progressively dominate the dispersion process. If the spectra in the model and prototype are of a similar shape, then similarity would be achieved. However, for a given turbulent flow a decrease in Reynolds number (hence, wind velocity) decreases the range (or energy) of the high frequency end of the spectrum. Fortunately, due to the nature of the filter function, the high frequency (small wave length) components do not contribute significantly to the dispersion. There would be, however, some critical Reynolds number below which too much of the high frequency turbulence is lost. If a study is run with a Reynolds number in this range, similarity may be impaired.

The ambient flow field also affects the plume trajectories and consequently similarity between model and prototype is required. The mean flow field will become Reynolds number independent if the flow is fully turbulent (Schlichting, 1968; Sutton, 1953). The critical Reynolds number for this criteria to be met is based on the work of Nikuradse as summarized by Schlichting (1968) and is given by:

$$(\text{Re})_{k_s} = \frac{k_s u_*}{\nu} > 75$$

or assuming $k_s = 30 z_o$

$$(\text{Re})_{z_o} = \frac{z_o u_*}{\nu} > 2.5.$$

In this relation k_s is a uniform sand grain height and z_o is the surface roughness factor. $(\text{Re})_{z_o}$ values were computed and will be discussed in Section 5.

The Rossby number, Ro , is a quantity which indicates the effect of the earth's rotation on the flow field. In the wind tunnel, equal Rossby numbers between model and prototype cannot be achieved. The effect of

the earth's rotation becomes significant if the distance scale is large. Snyder (1979) puts a conservative cutoff point at 5 km for diffusion studies. For this particular study, the maximum range over which the plume is transported is less than 9 km in the horizontal and 400 m in the vertical. The horizontal distance is larger than the cutoff recommended by Snyder but for rough terrain a larger distance is acceptable.

When equal Richardson numbers are achieved, equality of the Eckert number between model and prototype cannot be attained. This is not a serious compromise since the Eckert number is equivalent to a Mach number squared. Consequently, the Eckert number is small compared to unity for laboratory and atmospheric flows.

3.3 Equal Scaling Parameters

Since air is the transport medium in the wind tunnel and the atmosphere, near equality of the Prandtl number is assured.

The remaining relevant parameters are the velocity ratio,

$$R = \frac{u_s}{u_a} \quad (3.13)$$

Froude number,

$$Fr_\Gamma = \frac{u_s}{\sqrt{g\Gamma D}} \quad (3.14)$$

density ratio,

$$\Gamma = \frac{\rho_a - \rho_s}{\rho_s}$$

and Richardson number,

$$Ri = \frac{g}{\bar{T}} \frac{(T_\infty - T_o)\delta}{u_\infty^2} \quad (3.15)$$

Since the model scale was chosen to be 1:3072 for this study, matching of all of the above parameters would result in low tunnel operating

speeds (hence low Reynolds number). For example, if a 10 m/s wind were to be simulated a corresponding speed in the wind tunnel would be 0.18* m/s. In order to obtain higher tunnel operating speeds an alternate set of similarity criteria was used as recommended in Snyder (1979). The two parameters set equal in model and prototype are a momentum ratio, M_o , defined by,

$$M_o = \left(\frac{\rho_s}{\rho_a} \right) \left(\frac{u_s D}{u_a H_s} \right)^2 = (1 - \gamma) \left(\frac{RD}{H_s} \right)^2 \quad (3.16)$$

and a Buoyancy ratio, B_o , defined as follows,

$$B_o = \frac{gD^2 \gamma u_s}{u_a^3 H_s} = \frac{R^3}{Fr^2} \frac{D}{H_s} \quad (3.17)$$

where

$$\gamma = \frac{\rho_a - \rho_s}{\rho_a}$$

$$Fr = \frac{u_s}{\sqrt{g\gamma D}}$$

Use of these two parameters as similarity variables allows the relaxation of the density ratio, stack diameter, Froude number and velocity ratio.

Justification of the parameters is due to Briggs (1969, 1975) who developed an analytical expression for plume rise which is given by:

$$\left(\frac{\Delta h}{H_s} \right)^3 = \left(\frac{3}{4\beta_1^2} \right) M_o \left(\frac{x}{H_s} \right) + \frac{3}{8\beta_2^2} B_o \left(\frac{x}{H_s} \right)^2 \quad (3.18)$$

where Briggs (1975) gives:

$$\beta_1 = 0.5 \text{ and } \beta_2 = 1/3 + \frac{1}{R} .$$

His development used the equations of motion and energy with various simplifying assumptions. The above equation has been tested against field

*Note the following scaling relation has been applied:

$$u_m = u_p \sqrt{\frac{L_m}{L_p}}$$

and laboratory observations and has shown acceptable agreement in many cases (Briggs, 1975). The same plume rise will be predicted for a source if M_o and B_o are equal for the two cases; that is, if we assume β_1 and β_2 are also equal. The entrainment parameters will be equal if the flow is fully turbulent both in the plume and surrounding ambient fluid. Thus for the plume rise in the model and full-scale to be equal only the parameters M_o and B_o need be equated.

The ambient stability was simulated by cooling the model surface and heating the free stream air in the tunnel to achieve the maximum $T_\infty - T_o$. Thereafter u_∞ was adjusted to a speed where local slope winds were not evident. The Richardson number computed in the tunnel will then match a similar case in the field.

In summary the following similarity relations were applied for this study:

$$1) \quad M_o = (1 - \gamma) \left(R \frac{D}{H_s} \right)^2; \quad (M_o)_m = (M_o)_p$$

$$2) \quad B_o = \frac{R^3}{Fr^2} \frac{D}{H_s}; \quad (B_o)_m = (B_o)_p$$

$$3) \quad Ri = \frac{g}{T} \frac{(T_\infty - T_o)\delta}{u_\infty^2}; \quad (Ri)_m = (Ri)_p$$

$$4) \quad Re_{k_s} = \frac{u_* k_s}{\nu}; \quad 20 < Re_{k_s} < 70$$

$$5) \quad \text{Similar geometric dimension} \quad \left[\text{i.e.,} \left(\frac{D}{H_s} \right)_m = \left(\frac{D}{H_s} \right)_p \right]$$

$$6) \quad \text{Equality of dimensionless boundary conditions.}$$

Table 3.1 gives the model and full scale conditions that were developed by using these scaling criteria. The length scaling was 1:3072. The stack diameters were not scaled but were distorted while assuring that M_o and B_o were equal in model and full scale.

4. EXPERIMENTAL METHOD

4.1 Summary

The objective of this study is to evaluate the transport and diffusion of plumes emitted from the ASARCO and Kennecott stacks under a stable atmospheric condition. To meet this objective a 1:3072 scale model of the ASARCO and Kennecott stacks and topography was constructed and placed in the Colorado State University Meteorological Wind Tunnel. A stable boundary layer was developed over the topographic surface and tracer gas releases were made through the model stacks simulating a free stream wind speed of 10 m/s and Richardson number of 0.53 (Pasquill-Gifford E). The model operating conditions and those of the prototype are given in Table 3.1.

A stable boundary layer characteristic of the smelter vicinity was established and velocity and temperature profile measurements were made at 7 locations. The profiles were analyzed to 1) assess the effect of the terrain upon the flow field, 2) verify that the boundary layer was representative of the site, and 3) document the wind-tunnel flow characteristics.

After completing the velocity measurements a metered quantity of buoyant gas was allowed to flow from the model stacks and the wind tunnel was adjusted to simulate the desired ambient wind speed. Ground-level concentration measurements for each test were then obtained.

To qualitatively document the flow pattern the plume was made visible by passing the gas mixture through titanium tetrachloride prior to emission from the model stacks. Stills (color and black and white) and motion pictures of the tests were obtained.

A more detailed description of every facet of the study will now be given.

4.2 Scale Model and Wind Tunnel

A 1:3072 scale model of the topography in the vicinity of the ASARCO stacks was constructed to be positioned in the Colorado State University Meteorological Wind Tunnel (MWT) shown in Figure 4-1. The topographic strip that was constructed is shown in Figure 4-2. Also shown in the figure are various reference points at which velocity and temperature measurements were obtained. These points will be referred to in the results section of the report.

Construction of the topographic model entailed a two-step process. The first step involved constructing a styrofoam model. United States Geological Survey maps were enlarged and used as patterns from which the styrofoam was cut. The second phase of construction entailed constructing a wood-ribbed frame. Next, thin aluminum foil was placed on the styrofoam model and molded to fit the terrain contours. Once a strip was molded it was placed onto the wood frame and fastened. This hollow platform was then placed on the cooling plates that are permanently installed in the wind tunnel.

This wind tunnel, especially designed to study atmospheric flow phenomena (Cermak, 1958; Plate and Cermak, 1963), incorporates special features such as an adjustable ceiling, a rotating turntable, temperature controlled boundary walls, and a long test section to permit adequate reproduction of micrometeorological behavior. Mean wind speeds of 0.1 to 39.6 m/s in the MWT can be obtained. Boundary layer thickness up to 1.2 m can be developed naturally over the downstream 6.1 m of the MWT test section. Thermal stratification in the MWT is provided by the heating and cooling systems in the section passage in the test-section floor.

Installed aluminum cooling plates were cooled and the free-stream air (air entering the test section) temperature was controlled to obtain the desired thermal stratification. Pictures of the aluminum panel and terrain inside the MWT are shown in Figure 4-3.

4.3 Flow Visualization

The purpose of this phase of the study is to visually assess the transport of the plumes released from the stacks. The data collected consist of a series of photographs of the smoke emitted from each stack for the conditions enumerated in Table 3.1.

The smoke was produced by passing compressed air through a container of titanium tetrachloride located outside the wind tunnel and transported through the tunnel wall by means of a Tygon tube terminating at the stack inlets. The plume was illuminated with high intensity lamps and a visible record was obtained by means of black and white photographs.

A series of 16 mm motion pictures was taken of all tests. A Bolex movie camera was used with a speed of 24 frames per second. The movies consisted of taking an initial close-up of the smoke release after which the camera was panned from the model stacks to approximately 9 km down-wind in the prototype.

4.4 Gas Tracer Technique

The purpose of this phase of the experimental study is to provide quantitative information on the transport and dispersion of the plume emitted from the stacks. Specifically, this phase must demonstrate the magnitude of the SO_2 concentration at the ground level. To meet this goal a comprehensive set of concentration measurements was taken.

An array of 24 sampling tubes was run into the tunnel under the model terrain and fastened to brass tubes having outlets at the model

surface as well as a sampling rake that was set on the ground to obtain supplemental data. The location of these points is shown in Figure 4-4.

The test procedure consisted of: 1) setting the proper tunnel wind speed, 2) releasing a metered mixture of source gas of the required density from the release stacks, 3) withdraw samples of air from the tunnel at the locations designated, and 4) analyze the samples with a flame ionization gas chromatograph (FIGC). Photographs of the sampling system and gas chromatograph are shown in Figure 4-5. The samples were drawn into each syringe over a 5 minute time period and consecutively injected into the FIGC.

The procedure for analyzing air samples from the tunnel was as follows: 1) a 2 cc sample volume drawn from the wind tunnel is introduced into the flame ionization detector (FID), 2) the output from the electrometer (in microvolts) is sent to the Hewlett Packard 3380 Integrator, (HP 3380) 3) a digital record is integrated and an ethane concentration determined by multiplying the integrated signal (μvs) times a calibration factor ($\text{ppm}/\mu\text{vs}$), and 4) a summary of the integrator analysis (ethane concentration, peak height, integrated voltage, etc.) is printed out on the integrator at the wind tunnel. Prior to any data collection a known concentration of tracer was introduced into the FID to determine the calibration factor.

The FID operates on the principle that the electrical conductivity of a gas is directly proportional to the concentration of charged particles within the gas. The ions in this case are formed by the effluent gas being mixed in the FID with hydrogen and then burned in air. The ions and electrons formed enter an electrode gap and decrease the gap resistance. The resulting voltage drop is amplified by an electrometer

and fed to the HP3380 integrator. When no effluent gas is flowing, a carrier gas (nitrogen) flows through the FID. Due to certain impurities in the carrier some ions and electrons are formed creating a background voltage or zero shift. When the effluent gas enters the FID the voltage increases above this zero shift in proportion to the degree of ionization or correspondingly the amount of tracer gas present. Since the chromatograph² used in this study features a temperature control on the flame and electrometer, there is very low zero drift. In case of any zero drift the HP3380 which integrates the effluent peak also subtracts out the zero drift.

The lower limit of measurement (an equivalent SO₂ concentration of approximately 0.001 ppm) is imposed by the instrument sensitivity and the background concentration of tracer within the air in the wind tunnel. Background concentrations were measured and subtracted from all data quoted herein.

The wind-tunnel concentration data for all tests in this report are presented in the form of a full-scale equivalent SO₂ concentration. To compute the full-scale concentration $(\chi_p)_{SO_2}$ a dimensionless concentration K from the wind-tunnel results is computed as follows:

$$K = \frac{\chi u_{\infty} \delta^2}{\chi_0 V} \quad (4.1)$$

where χ is the observed tracer concentration less the background, χ_0 is the source strength of the tracer gas, u_{∞} is the free stream velocity, at a height δ above the ASARCO stack, V the volume flow rate and δ is 0.20 m.

²A Hewlett-Packard 5700 gas chromatograph was used in this study.

To determine a corresponding full-scale concentration from the model K values, the K-model (K_m) is set equal to K-prototype (K_p). Equality of these two parameters can be verified by considering the equation for conservation of mass, or,

$$\left[\int_{-\infty}^{\infty} \int \frac{\chi u_{\infty}}{\chi_o V} dydz \right]_m = \left[\int_{-\infty}^{\infty} \int \frac{\chi u_{\infty}}{\chi_o V} dydz \right]_p = 1.$$

Since $(dy)_m = \frac{(\delta)_m}{(\delta)_p} (dy)_p$ and $(dz)_m = \frac{(\delta)_m}{(\delta)_p} (dz)_p$, the equation

can be rearranged to give

$$\int_{-\infty}^{\infty} \int \left[\left(\frac{\chi u_{\infty}}{\chi_o V} \right)_p - \left(\frac{\chi u_{\infty}}{\chi_o V} \right)_m \frac{(\delta^2)_m}{(\delta^2)_p} \right] (dydz)_p = 1.$$

For this equality to be true requires

$$\left(\frac{\chi u_{\infty}}{\chi_o V} \right)_p = \left(\frac{\chi u_{\infty}}{\chi_o V} \right)_m \frac{(\delta^2)_m}{(\delta^2)_p}$$

or

$$\left(\frac{\chi u_{\infty} \delta^2}{\chi_o V} \right)_m = \left(\frac{\chi u_{\infty} \delta^2}{\chi_o V} \right)_p ; K_m = K_p.$$

Solving for χ_p yields the following equation which is used in this report to calculate prototype concentrations

$$(\chi_p)_{SO_2} = K_m \left[\frac{\chi_o V}{u_{\infty} \delta^2} \right]_p. \quad (4.2)$$

- Averaging Time

Generally, steady-state average concentrations measured in the wind tunnel are thought to correspond to a 10- or 15-minute average in the atmosphere (Snyder, 1979). This line of reasoning is based on the observed energy spectrum of the wind in the atmosphere. This spectrum shows a null in the frequency range from 1 to 3 cycles per hour. Frequencies below this null represent meandering of the wind, diurnal fluctuations, and passage of weather systems and cannot be simulated in the wind tunnel. The frequencies above this null represent the fluctuations due to roughness, buildings and other local effects and are well simulated in the tunnel. This part of the spectrum will be simulated in the tunnel as long as the wind direction and speed characteristics remain stationary in the atmosphere which is typically 10 to 15 minutes. At many locations, however, persistent winds of three or more hours may occur. For these cases, the wind tunnel averaging time would correspond to the atmospheric averaging time. For the more typical cases, the wind-tunnel results would have to be corrected for the large-scale motion using power law relations such as given by Hino (1968) or Turner (1970).

4.5 Velocity and Temperature Measurements

Vertical profiles of mean velocity and temperature were obtained under a stable condition. The measurements were performed to 1) quantitatively assess the flow patterns over the simulated terrain, 2) monitor and set flow conditions, 3) document the condition in the wind tunnel, and 4) document characteristics of the thermal boundary layer. The velocity measurements were obtained with a Datametrics probe (Datametrics Linear Flow Meter, Model 800 LV) that is accurate to within 1 cm/sec

down to 2 cm/sec. Temperature was measured with a Yellow Springs, Inc. Precision Thermistor and a YSI Tele-Thermometer (Model 42SC).

The Datametrix probe works in the following manner. Two stainless steel wires are mounted on needle supports and exposed to the flow. One is called the "hot" filament and the other the "cold" filament. The Model 800 LV circuit automatically maintains enough electrical current in the hot filament to keep its operating temperature higher than the absolute temperature of the cold filament by a fixed ratio (about 1.3), resulting in a hot-wire temperature about 150^o F above the cold wire. When the flow rate is zero, the voltage is zero at the output receptacle. When the flow rate increases, the electrical current required to keep the hot filament hot automatically increases. This increase causes a voltage increase at the output receptacle. A built-in linearizer circuit is adjusted at the factory to assure that the output voltage is linearly proportioned to flow rate (Datametrix ITE Imperial Corp., 1973).

A total of seven velocity and temperature profiles were measured at various locations as shown in Figure 4-2. The manner of collecting the data was as follows:

- 1) The Datametrix probe and thermistor were attached to a carriage.
- 2) The bottom height of the profile was set to the desired initial height.
- 3) A vertical distribution of velocity and temperature was obtained using a vertically traversing mechanism.
- 4) The signals from the anemometer were fed directly to a Hewlett-Packard Series 1000 Real Time Executive Data Acquisition System.
- 5) Samples were stored digitally in the computer at a rate of approximately 30 samples per second, and

- 6) The computer program converted each voltage E into a velocity (m/s) using the equation:

$$u = E * C$$

where C is the calibration constant converting volts to velocity.

At this point the program computes several useful quantities using the following equations:

$$\bar{u} = 1/N \sum_{i=1}^N u_i \quad (4.3)$$

$$\overline{u'^2} = \frac{1}{N-1} \sum_{i=1}^N (u_i - \bar{u})^2 \quad (4.4)$$

where N is the number of velocities considered (typically a 30-second average was taken, hence 900 samples were obtained). The mean velocity and turbulence intensity at each measurement height were stored on a file in addition to being returned to the operator at the wind tunnel on a remote terminal. The temperature data were recorded by typing the indicated temperature from the Yellow Springs thermistor on the computer sheet at the remote terminal.

To check the temperature distribution on the surface of the aluminum shell model thermistors were placed at 7 points on the model. The temperature at each point and the relative location is given with the results discussed in Section 5. The mean temperature for the 7 points is 8.0° C, the high value 11.5° C, and the low value 4.5° C.

5. RESULTS

5.1 Velocity and Temperature Measurements

Velocity and temperature measurements were obtained to 1) establish the correct operating speeds in the tunnel, and 2) document the flow conditions in the wind tunnel. To meet this objective a total of seven vertical profiles of horizontal wind speed, turbulent intensity and temperature were obtained. For the tests the surface temperature was set to be approximately 8°C and free stream air 58°C. The free stream velocity was then set to be approximately 0.80 m/s over the ASARCO tall stack location. Free stream height was taken to be 0.2 m, AGL. Tables 5.1 through 5.7 give the mean velocity, turbulence intensity and temperature versus height for each measurement location. The locations are referenced in Figure 4-2.

To visually assess the flow characteristics over the model, Figures 5-1 through 5-7 were prepared. The mean velocity was nondimensionalized by the maximum velocity, u_m , for each profile and the temperature was nondimensionalized as follows:

$$T^* = \frac{T - T_0}{T_\infty - T_0}$$

where T^* is the dimensionless temperature, T the measured temperature at height z , T_0 the local surface temperature, and T_∞ the temperature at the top of the profile. The upper-level velocity and temperature ranged from 0.886 to 1.106 m/s and from 56.1°C to 60.1°C respectively as is evident in Figures 5-1 through 5-7.

To assess the flow characteristics in the wind tunnel the velocity profiles were analyzed to obtain the surface roughness length (z_0), the friction velocity (u_*), the turbulent Reynolds number (Re_{z_0}), the

reciprocal of the Monin-Obukhov length scale ($1/L$), and the power law exponent (n). The values of z_0 , u^* , $1/L$ were computed which gave the best fit (by least squares) to the following equation which is characteristic of atmospheric (Businger, 1972) and wind-tunnel flows (Cermak, 1974):

$$\frac{u}{u^*} = \frac{1}{k} \ln \left[\frac{z}{z_0} + \frac{4.7 z}{L} \right] \quad (5.1)$$

The power law exponent was computed by fitting the data by least squares to the following equation:

$$\frac{u}{u_\infty} = \left(\frac{z}{\delta} \right)^n \quad (5.2)$$

The power law exponent varies with stability in the atmosphere as given in Table 5.8.

The turbulent Reynolds number Re_{z_0} was computed for each profile and was used to assess whether the flow was fully turbulent. For fully turbulent flows $Re_{z_0} > 2.5$ (Schlichting, 1968; Sutton, 1953). The u^* and z_0 values used for computing Re_{z_0} were obtained from the least squares analysis. The root-mean-square error (e) between predicted and observed velocity was computed to assess the goodness of fit to equations 5.1 and 5.2.

Table 5.9 gives a summary of the analysis of each profile. The estimated values for z_0 , $1/L$, u^* , Re_{z_0} , n , e_{z_0} (the root-mean-square error between log-law and observation) and e_n (the root-mean-square error between power law and observation) are tabulated. The surface roughness ranged from 0.013 cm to 0.46 cm (0.4 to 14 m full scale) with a mean value of 0.155 cm (4.8 m full scale). As expected, the largest z_0 values were on the more rugged part of the terrain. In general the z_0 values are typical for rough terrain. The friction velocity ranged from 5.52 cm/s to 11.19 cm/s with an average value of 7.52 cm/s. The average turbulent

Reynolds number is 9.52, above the limit of 2.5 for fully turbulent flows. The power-law exponent (n) for the profiles ranged from 0.18 to 0.42 with an average value of 0.28. The large values of n are expected for a stable boundary layer as shown in Table 5.8. For the atmosphere and hilly terrain n varies from 0.26 to 0.52 for E and G stability respectively. Based on the power-law it appears a Pasquill category E was simulated. The l/L values vary from -0.55 to 0.80. A positive l/L indicates a stable stratification and a negative, unstable. The negative l/L occurs at Location 3 which is in very complex terrain and has a large z_0 . This indicates that the surface has enhanced the mixing and destabilized the flow at this location. All other points indicated a stable flow but l/L was generally smaller (less stable) for the locations that have a large z_0 .

In summary the results show that a stable boundary layer was simulated.

5.2 Plume Transport and Diffusion Results

● Photographic Results

A series of black and white photographs, color slides and motion pictures of the tests indicated in Table 3.1 were obtained to qualitatively document the dispersion patterns from the three stacks. Due to the low volume flows the black and white photographs were not of adequate quality to depict the motion. However, at a low tunnel speed -- which gives a higher plume rise and hence more contrast -- the plumes from the tall stacks were made visible. The photographs of these tests are shown in Figure 5-8. As can be noticed the rise from the ASARCO stack is substantially greater than the Kennecott stack. A better visual description of the dispersion from all three stacks for the conditions in Table 3.1 can be seen by viewing the motion picture.

- Concentration Measurement Results

The purpose of this phase of the study was to determine the relative contribution to the total SO_2 concentration due to each stack at the Montgomery Ranch monitoring site (MRS). To meet this goal concentration measurements were obtained at locations 7 through 12 shown in Figure 4-4. Location 10 was closest to the actual MRS. To more fully document the ground-level concentrations measurements were also taken at the other locations annotated in Figure 4-4. The procedures for collecting the data are given in Section 4.4.

As a review, a gas mixture with tracer included was released from the ASARCO stack (6.85% ethane mixture), Kennecott #1 (6.85% ethane mixture) and Kennecott #2 (4.45% propane mixture). Each release was made separately while maintaining the conditions given in Table 3.1. For each stack studied the test was repeated twice and an average concentration at each receptor computed. Tables 5.10 through 5.12 give the equivalent SO_2 concentration (model values converted to full scale using equation 4.2) for each run and the average used in subsequent discussions. The variation in concentration at the same location for Repeats 1 and 2 for each stack was the greatest for the tall stacks (ASARCO and Kennecott #1). The average deviation from the mean was about 30% for these runs. For the short stack (Kennecott #2) the deviation was on the average less than 5% at a fixed location for Repeat 1 and 2. The reason the taller stacks showed more variation for each repeat is because the edges of the plume, which are sporadic in nature, were being measured. For the short stack, on the other hand, close to a center line value was being measured since the release was near the surface.

To assess the relative impact of each plume at the Montgomery Ranch Station (MRS), Table 5.13 was prepared. This table gives the measured

equivalent SO_2 concentration at Locations 7 through 12 due to each stack individually and the total concentration. Also in the table are the percentages of total concentration due to each source, the average concentration and percentage at Locations 7 through 12, the emission rate for each stack and percent of total emissions for each stack. At Location 10, which is closest to MRS, the ASARCO stack contributes 29%, Kennecott #1 contributes 52%, and Kennecott #2 (6 tons per day sulphur emission rate) contributes 19% of the total SO_2 concentration of 0.077 ppm. The average contribution for Locations 7 through 12 is 30%, 48% and 22% for the respective sources ASARCO tall stack, Kennecott #1, and Kennecott #2. This result is in sharp contrast to the percent of total emissions. The ASARCO stack contributes 80%, the Kennecott tall stack 18%, and the Kennecott short stack 2%. If a 60 ton/day sulphur emission rate from Kennecott #2 is assumed the total SO_2 impact at receptor #10 is 0.21 ppm with respective contributions due to the ASARCO stack, Kennecott #1 and Kennecott #2 of 11%, 19% and 70%.

The concentration measurement results demonstrate that percent emission does not relate to the percent of ground-level concentration contribution. This result is predicted by the Gaussian diffusion equation (Turner, 1970). This equation shows that ground-level concentration is proportional to stack height as follows:

$$\chi \propto \exp \left[-\frac{1}{2} \left(\frac{h}{\sigma_z} \right)^2 \right].$$

Hence increasing stack height decreases ground-level concentrations exponentially. The results of this study further demonstrate the effect of this exponential relationship. A short stack which emits 2% of the total SO_2 contributes 22% of the ground-level concentration.

REFERENCES

- Briggs, G. A., Plume Rise, USAEC Critical Review Series, TID25075, Clearinghouse for Federal Scientific and Technical Information.
- Briggs, G. A., "Plume Rise Predictions," presented in Lectures on Air Pollution and Environmental Impact Analysis, sponsored by American Meteorological Society, September 29-October 3, 1975, Boston, Massachusetts.
- Cermak, J. E., "Applications of Fluid Mechanics to Wind Engineering," presented at Winter Annual Meeting of ASME, New York, November 17-21, 1974.
- Cermak, J. E., "Wind Tunnel for the Study of Turbulence in the Atmospheric Surface Layer," Fluid Dynamics and Diffusion Laboratory, Technical Report CER58-JEC42, Colorado State University, Fort Collins, Colorado, 1958.
- Csanady, G. T., Turbulent Diffusion in the Environment, D. Reidel Publishing Company, Doudrecht, Holland, 1973.
- Hewett, T. A., J. A. Fay, and D. P. Hoult, "Laboratory Experiments of Smokestack Plumes in a Stable Atmosphere," Atmospheric Environment, Vol. 3, pp. 767-789, 1971.
- Hinze, O. J., Turbulence, Second Edition, McGraw-Hill, Inc., 1975.
- Hoult, D. P., and J. Weil, "Turbulent Plume in a Laminar Cross Flow," Atmospheric Environment, 6:513-531, 1972.
- Pasquill, F., Atmospheric Diffusion, Second Edition, John Wiley and Sons, New York, 1974.
- Petersen, R. L., J. E. Cermak, R. N. Meroney, and E. L. Hovind, "A Wind Tunnel Study of Plume Rise and Dispersion Under Stable Stratification," Joint Conference on Applications of Air Pollution Meteorology, Salt Lake City, Utah, November 29-December 2, 1977.
- Plate, E. J., and J. E. Cermak, "Micro-meteorological Wind Tunnel Facility," Fluid Dynamics and Diffusion Laboratory, Technical Report CER63EJP-JEC9, Colorado State University, Fort Collins, Colorado, 1963.
- Schlichting, H., Boundary Layer Theory, McGraw-Hill, Inc., New York, 1968.
- Snyder, W. H., "Similarity Criteria for the Application of Fluid Models to the Study of Air Pollution Meteorology," Boundary Layer Meteorology, Vol. 3, pp. 113-134, 1972.

Snyder, W. H., "Guideline for Fluid Modeling of Atmosphere Diffusion," USEPA Office of Air, Noise and Radiation, Research Triangle Park, North Carolina 27711, Draft for Public Comment EPA-450/4-79-016, June, 1979.

Sutton, O. G., Micrometeorology, McGraw-Hill, Inc., New York, 1953.

Taylor, G. I., "Diffusion by Continuous Movements," Proceedings, London Meteorological Society, Vol. 20, pp. 196-211, 1921.

Touma, J. S., "Dependence of the Wind Profile Power Law on Stability for Various Locations," Journal of Air Pollution Control Association, Vol. 27, No. 9, 1977.

FIGURES

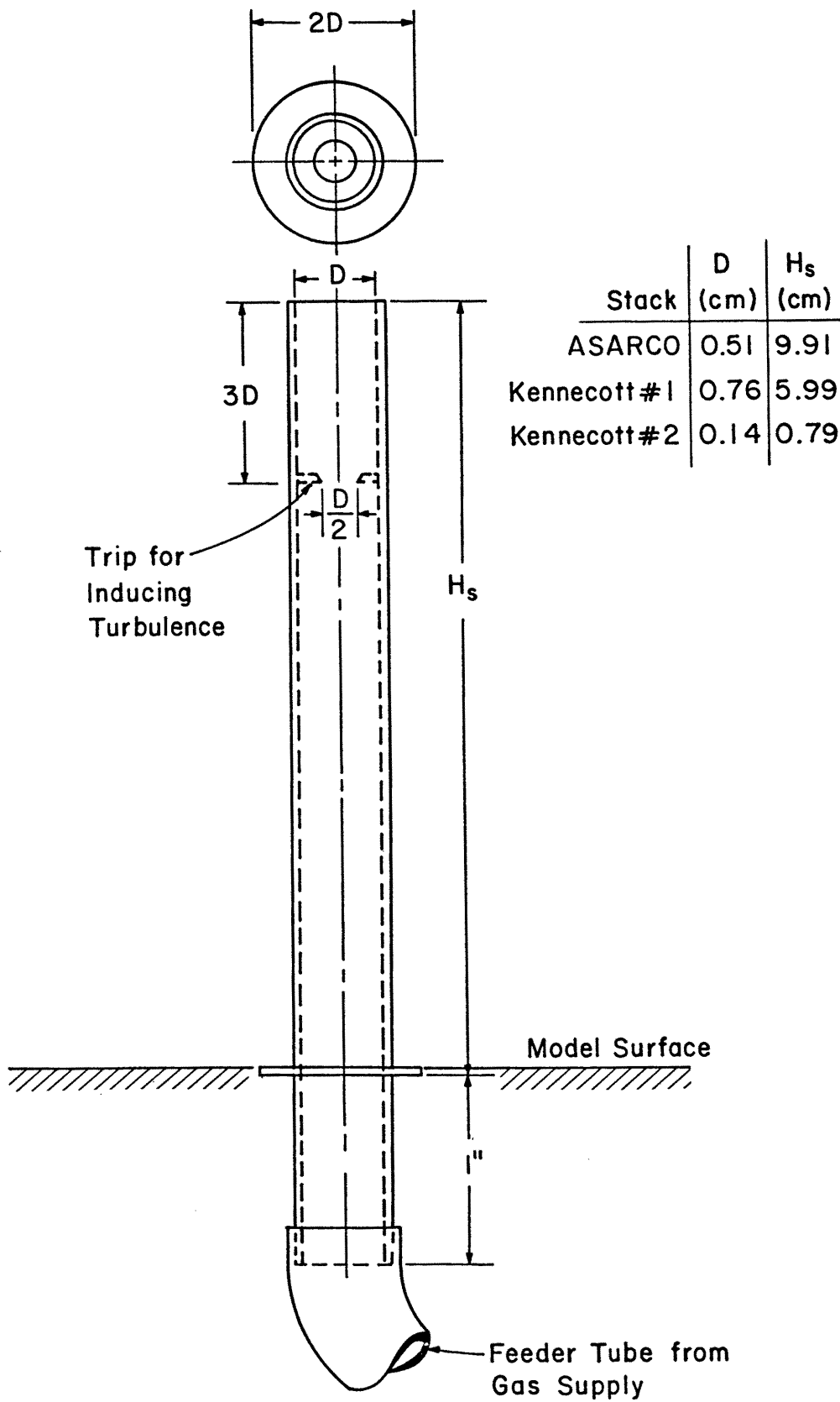
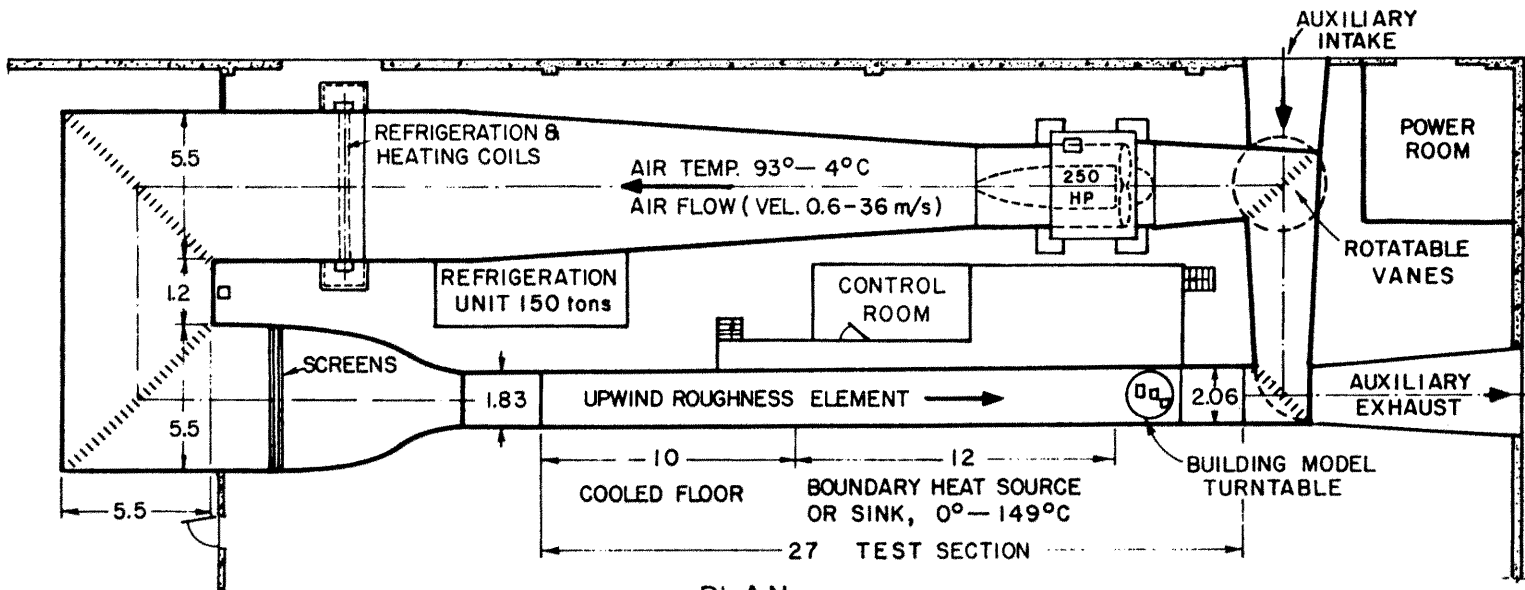
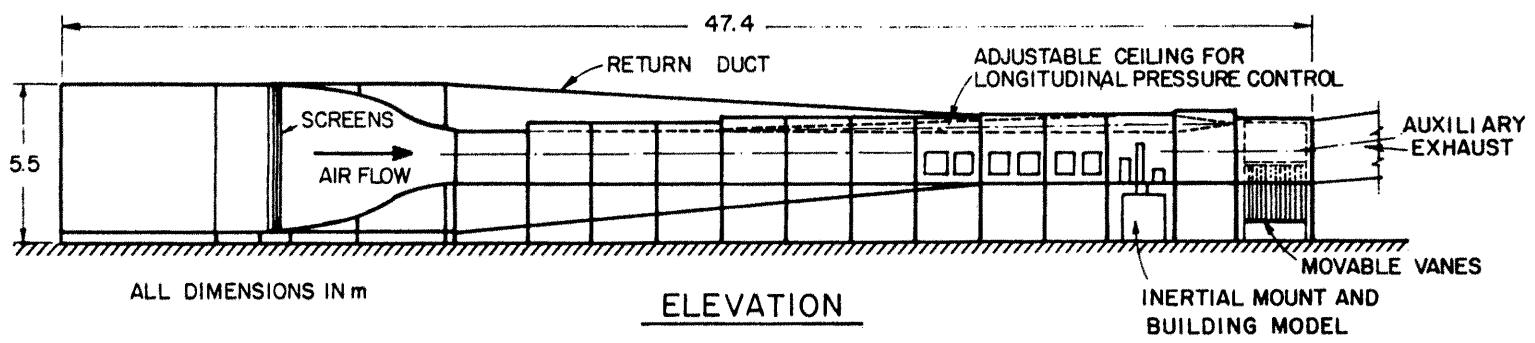


Figure 3-1. Drawing of Model Stack used for ASARCO Stable Wind Tunnel Tests.



PLAN



ELEVATION

Figure 4-1. Meteorological Wind Tunnel. Fluid Dynamics and Diffusion Laboratory. Colorado State University.

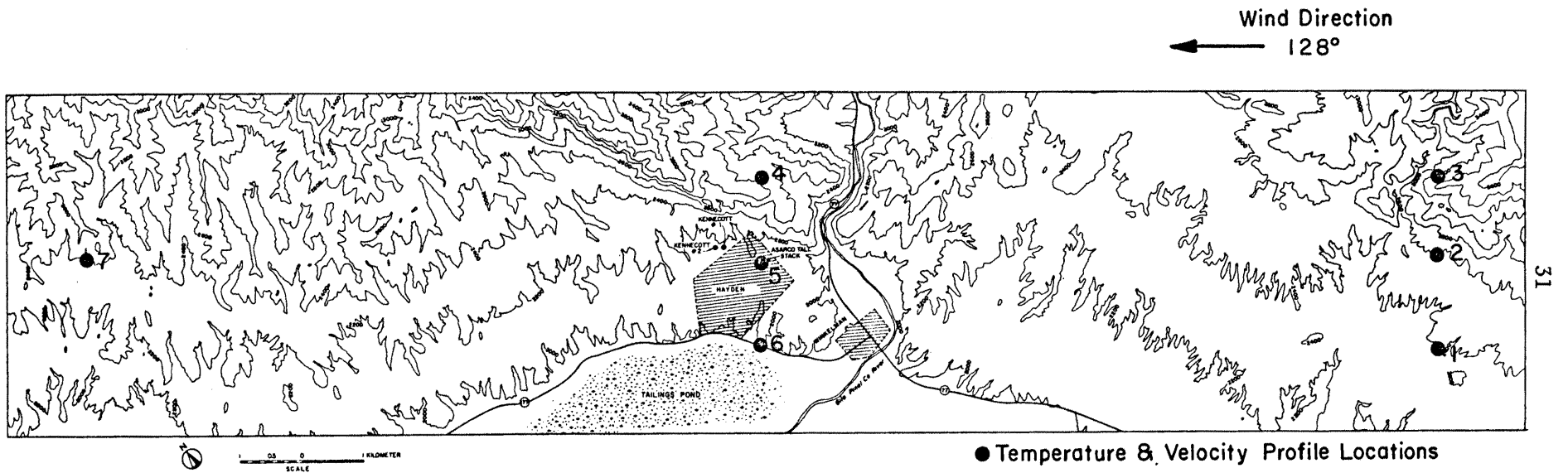
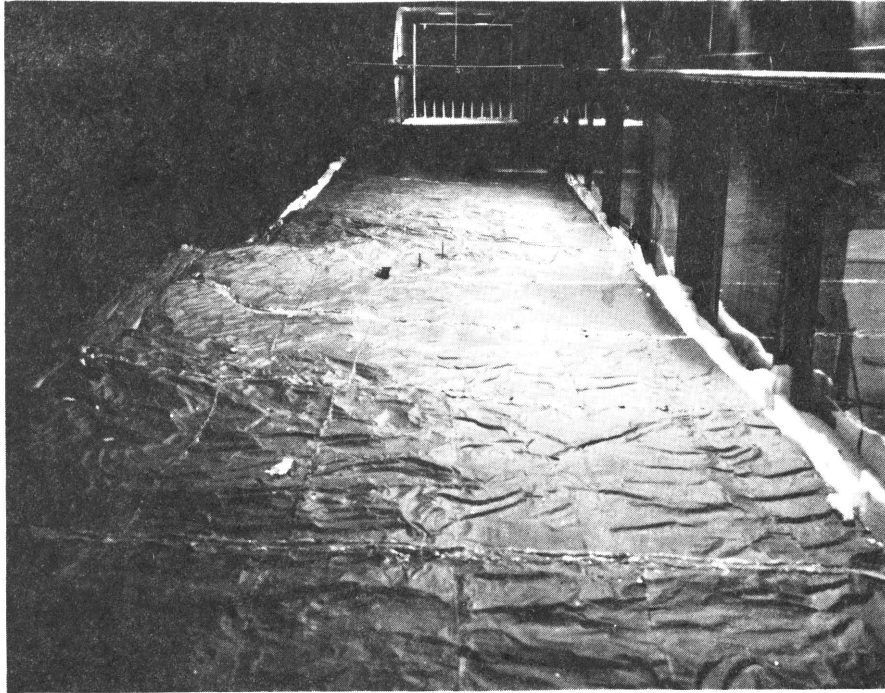
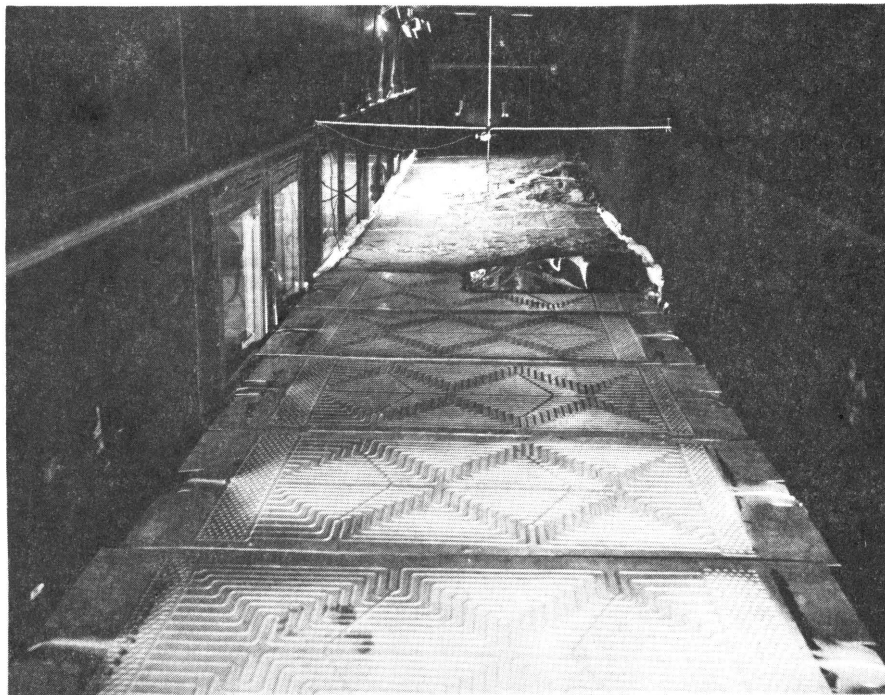


Figure 4-2. Topographic Map of the Area Modeled in the Wind Tunnel showing the Velocity and Temperature Profile Measurement Locations and the Stack Locations.



a)



b)

Figure 4-3. Photographs showing a) the Terrain in the Tunnel looking into the Flow and b) the Approach to the Model Terrain and the Upwind Cooling Plates.

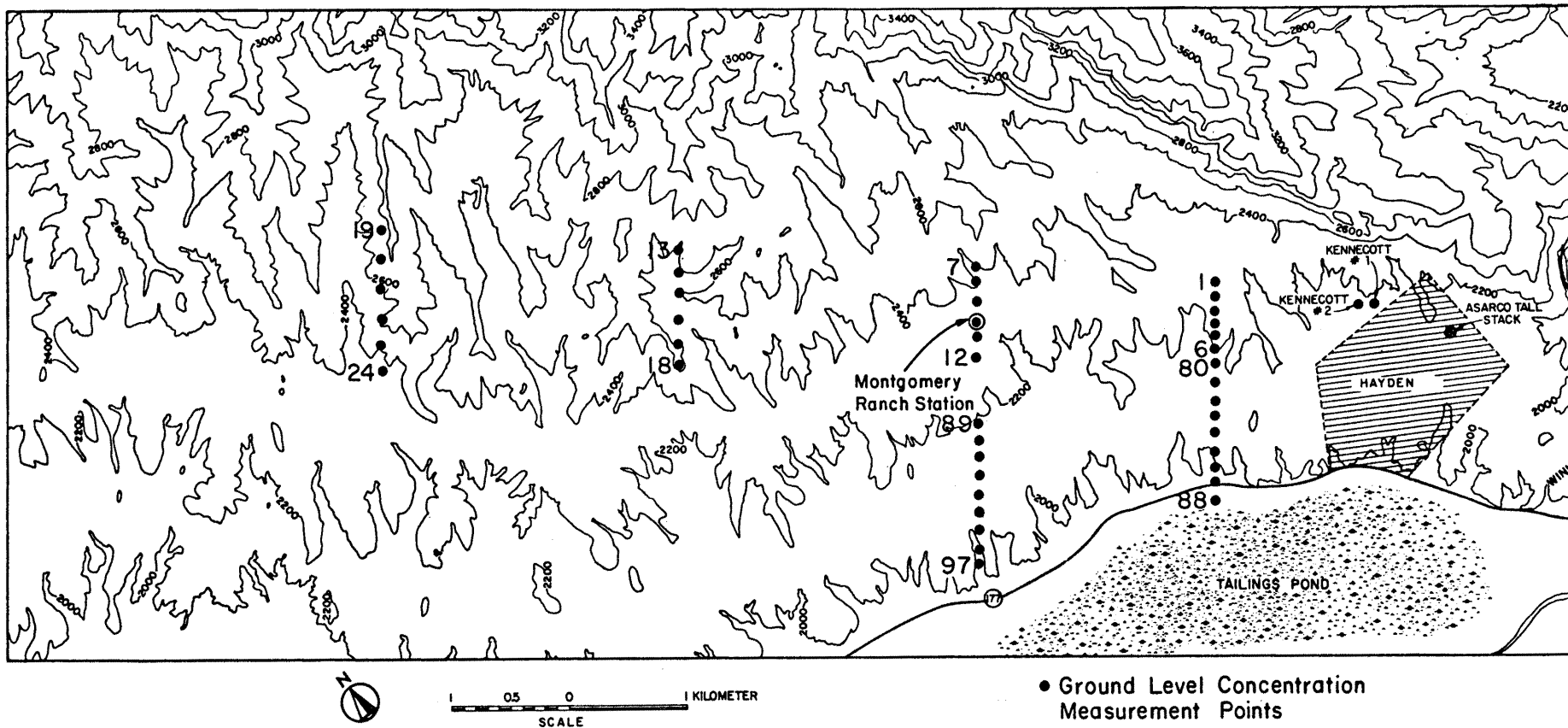
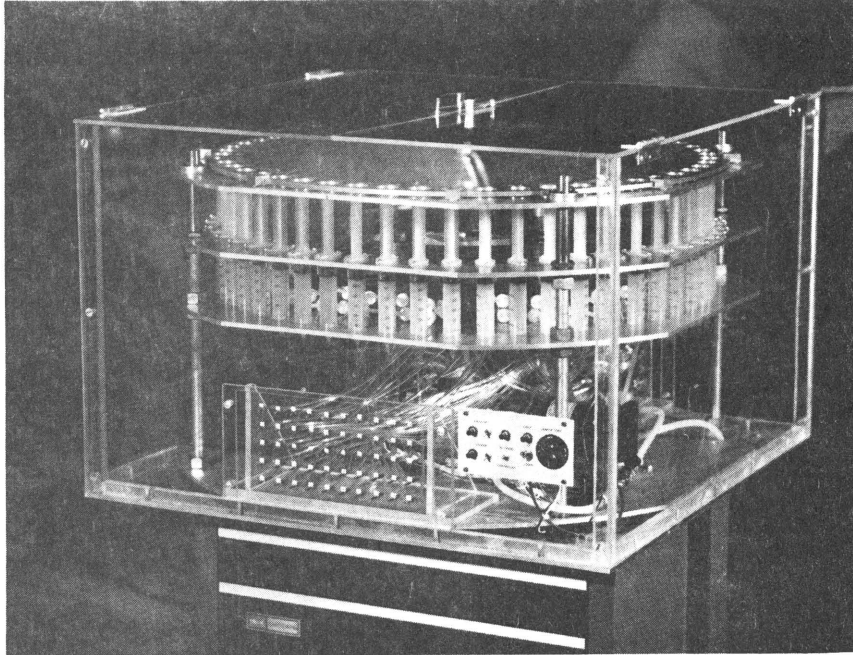
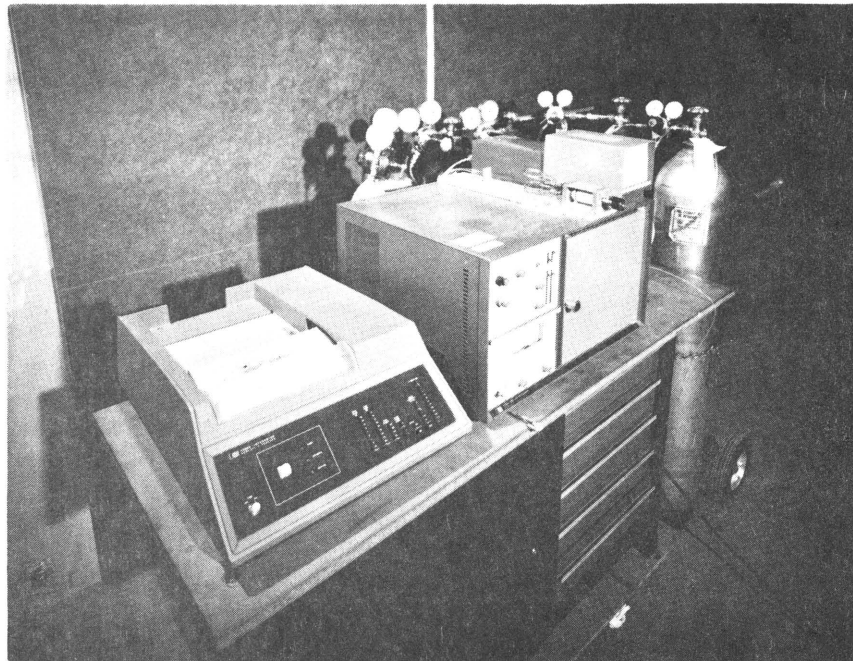


Figure 4-4. Map showing Ground-Level Concentration Sampling Locations and Location Number.



a)



b)

Figure 4-5. Photographs of a) the Tracer Gas Sampling System and b) the Hewlett Packard Gas Chromatograph and Integrator.

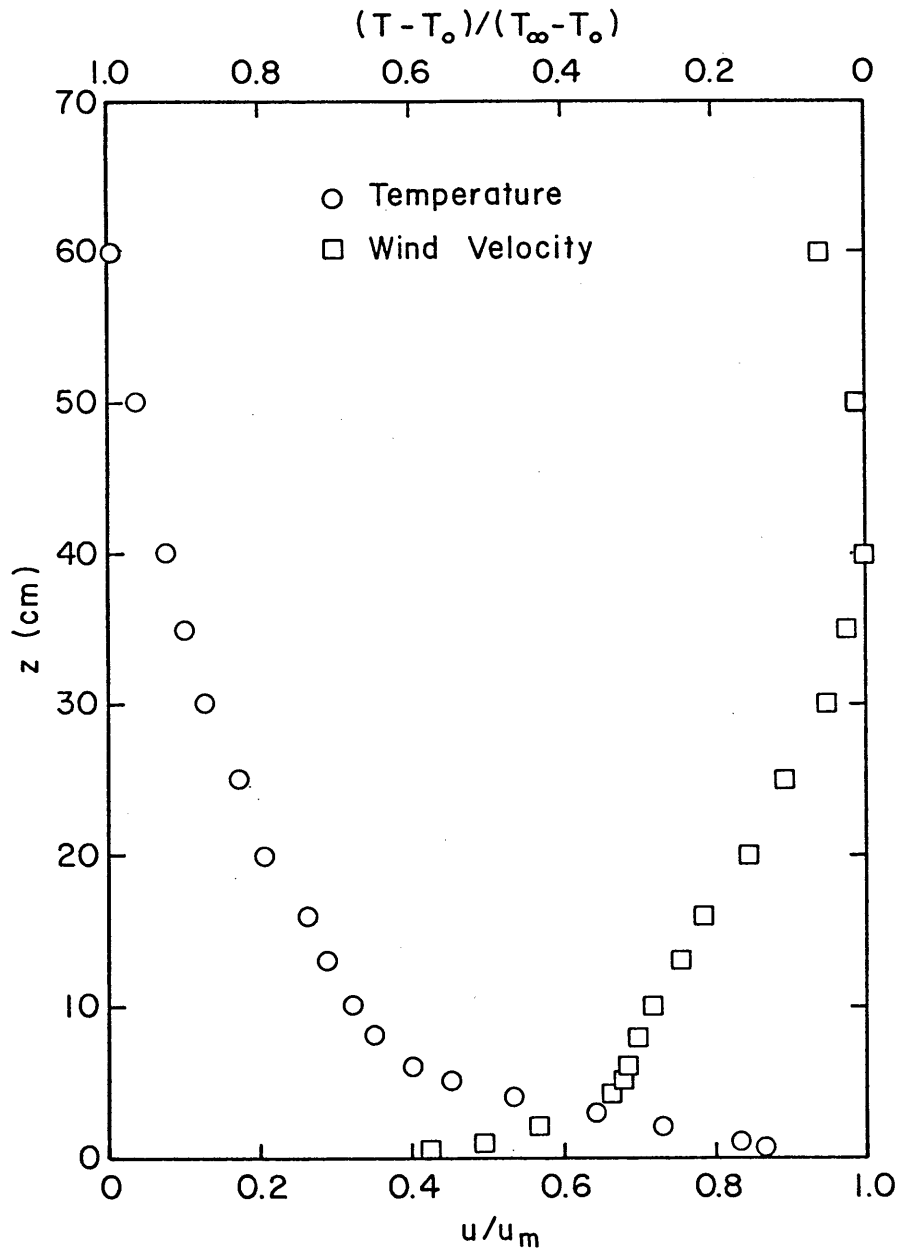


Figure 5-1. Dimensionless Velocity and Temperature Profile at Location No. 1 for $T_o = 6.5^{\circ}\text{C}$, $T_{\infty} = 57.2^{\circ}\text{C}$ and $u_m = 0.964$ m/sec.

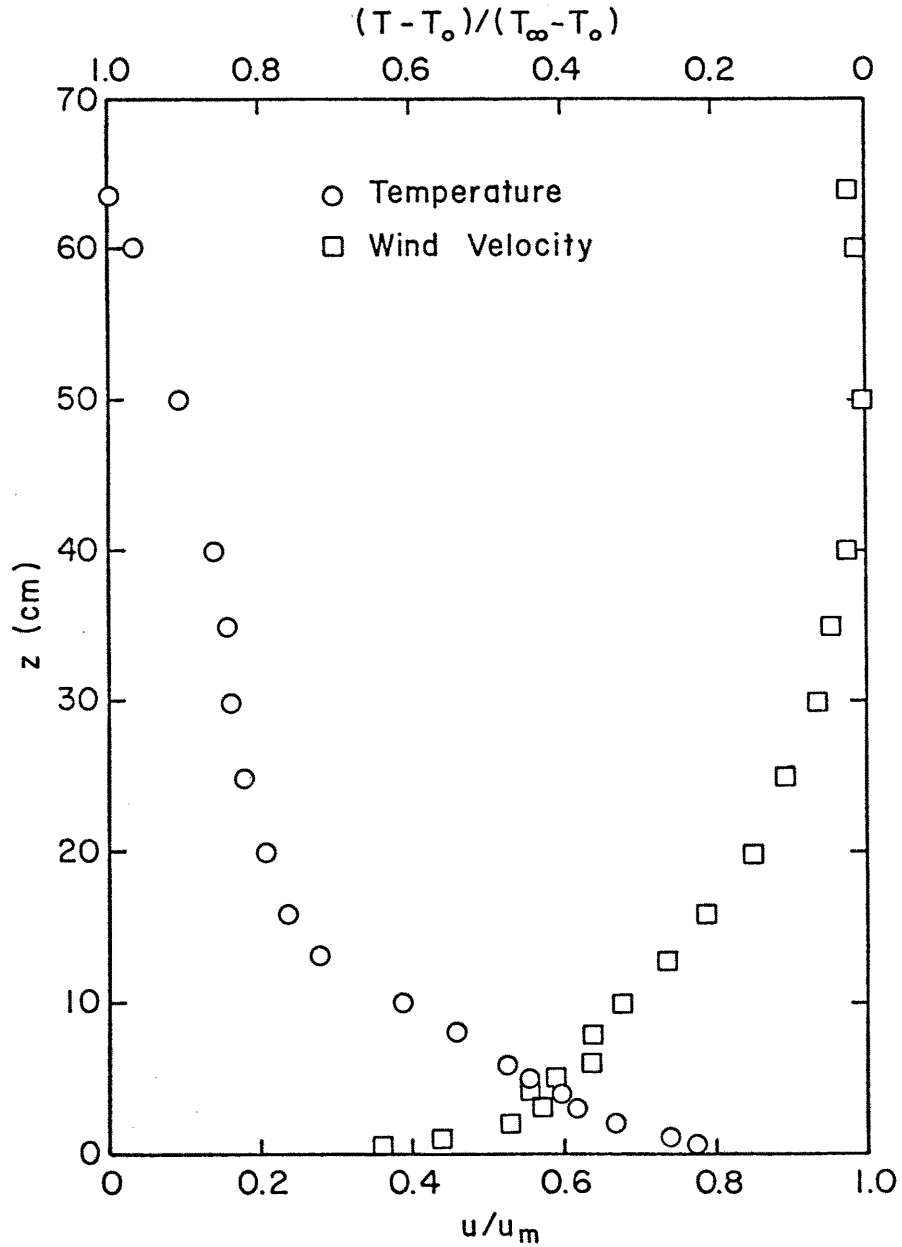


Figure 5-2. Dimensionless Velocity and Temperature Profile at Location No. 2 for $T_o = 10.5^\circ\text{C}$, $T_\infty = 60.1^\circ\text{C}$ and $u_m = 0.886$ m/sec.

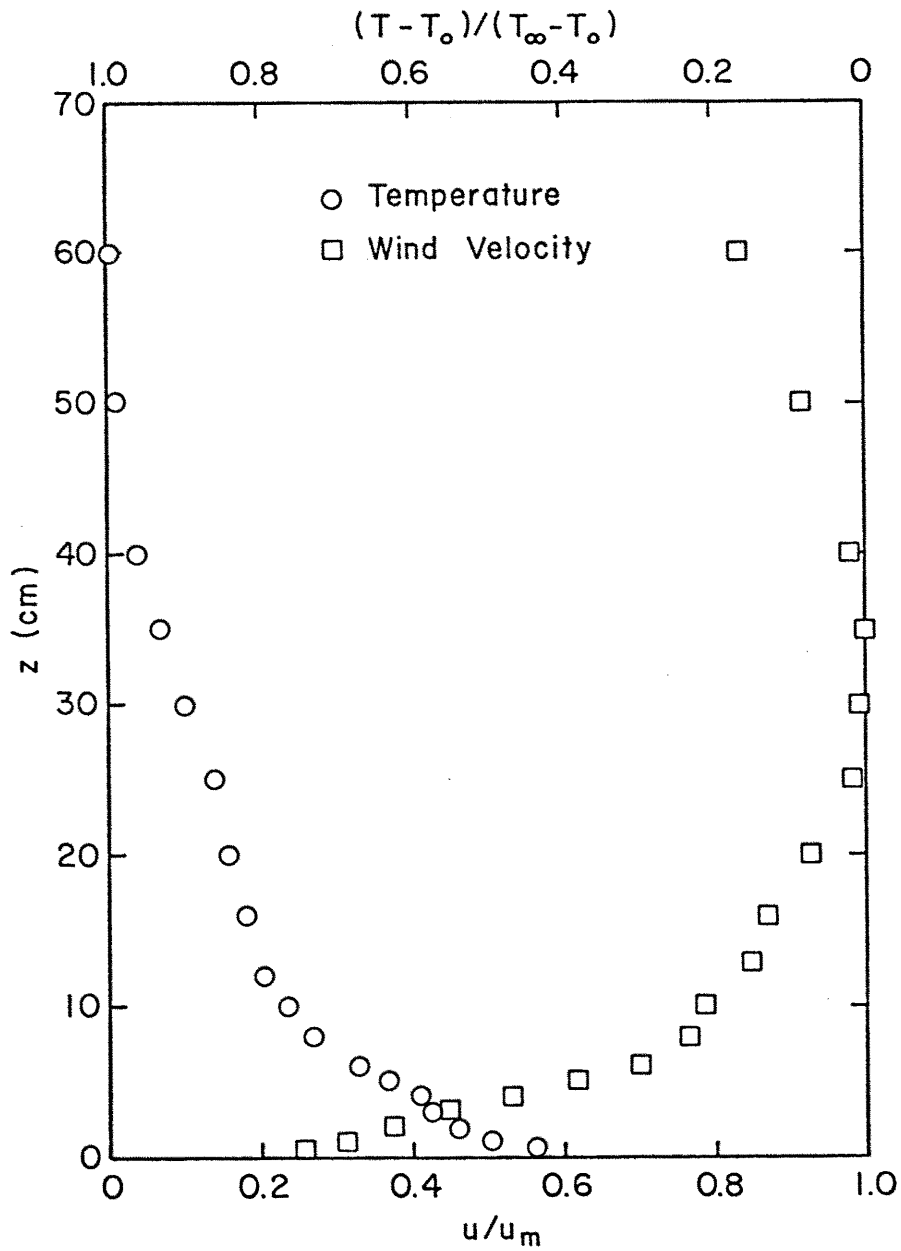


Figure 5-3. Dimensionless Velocity and Temperature Profile at Location No. 3 for $T_o = 11.5^\circ\text{C}$, $T_\infty = 59.0^\circ\text{C}$ and $u_m = 0.972$ m/sec.

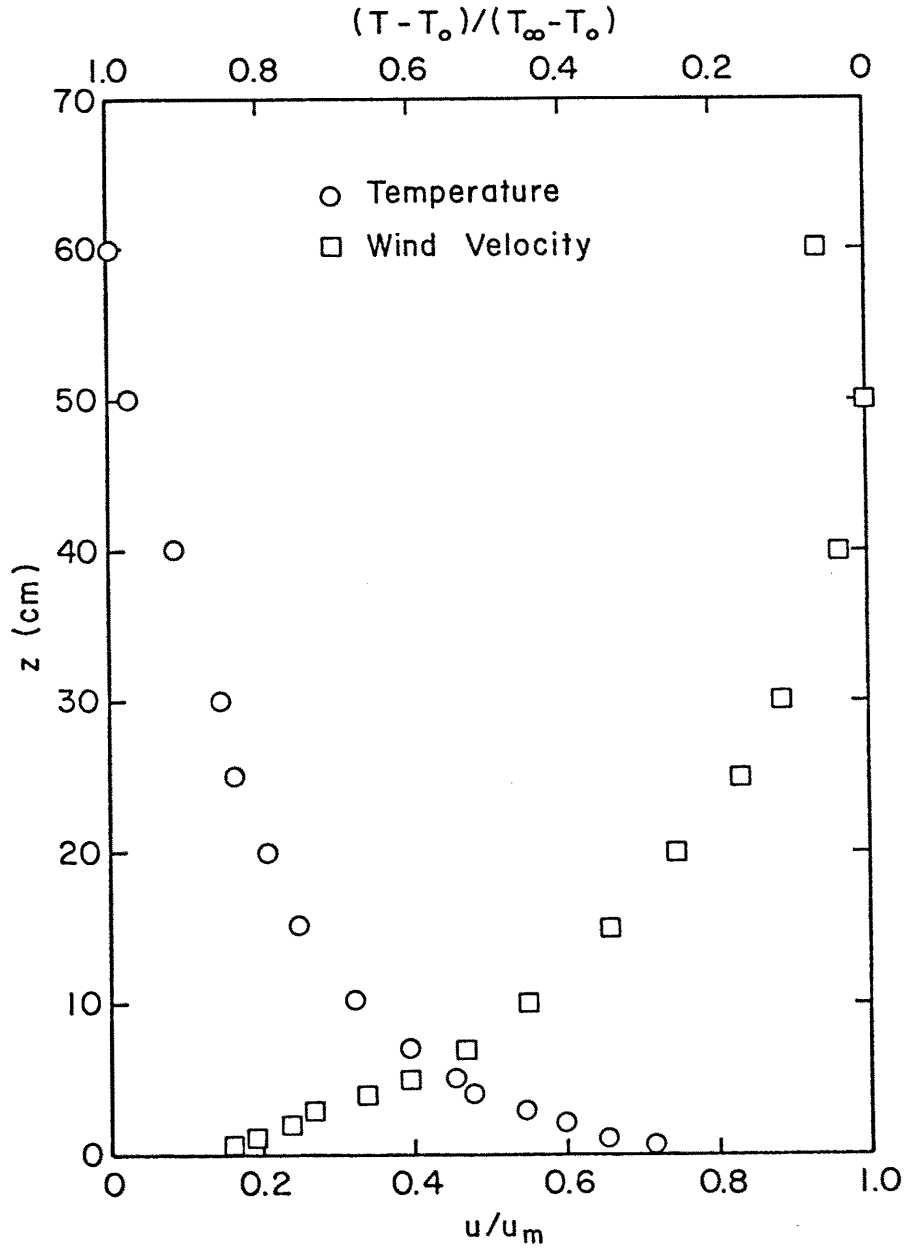


Figure 5-4. Dimensionless Velocity and Temperature Profile at Location No. 4 for $T_o = 9.1^\circ\text{C}$, $T_\infty = 57.4^\circ\text{C}$ and $u_m = 1.106 \text{ m/sec}$.

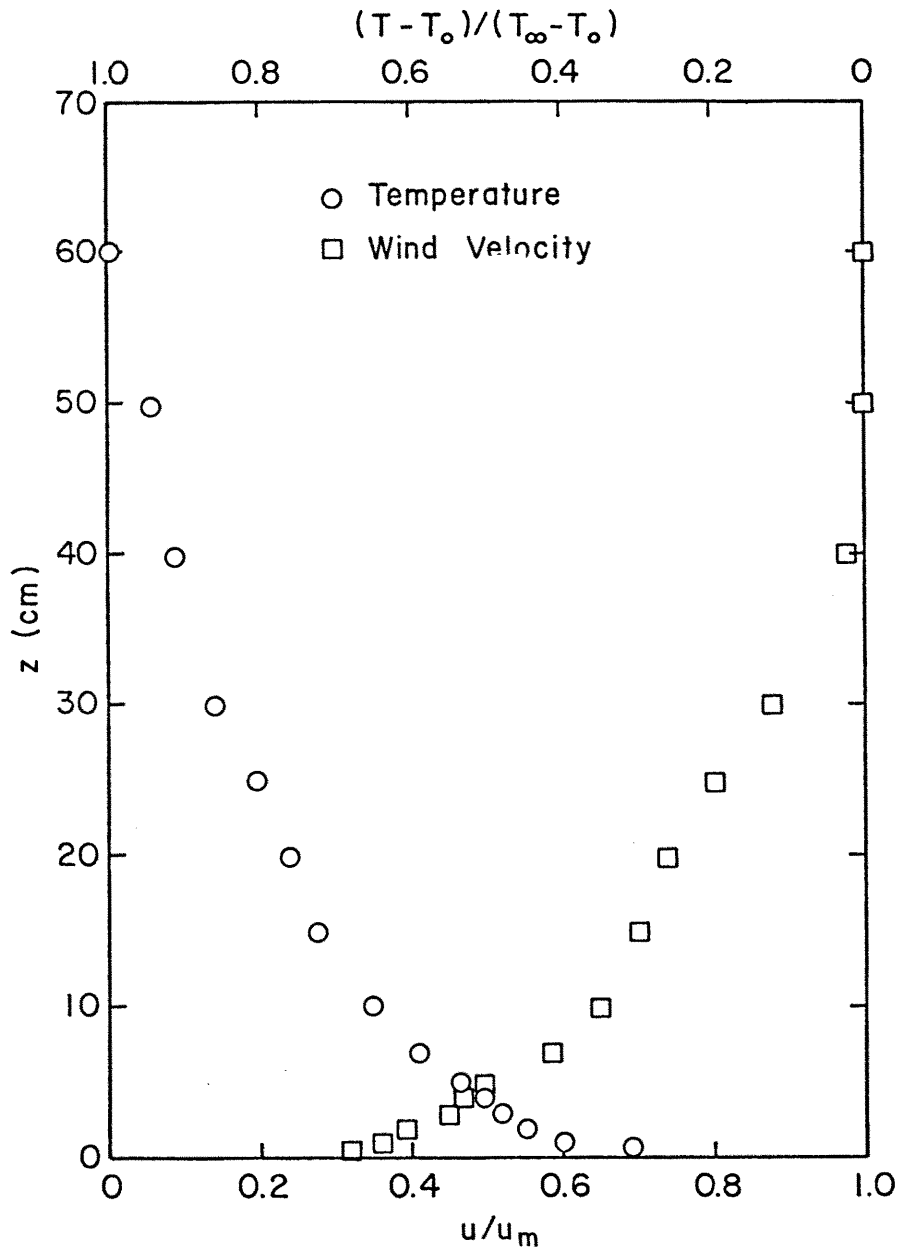


Figure 5-5. Dimensionless Velocity and Temperature Profile at Location No. 5 for $T_o = 8.2^\circ\text{C}$, $T_\infty = 56.7^\circ\text{C}$ and $u_m = 1.087$ m/sec.

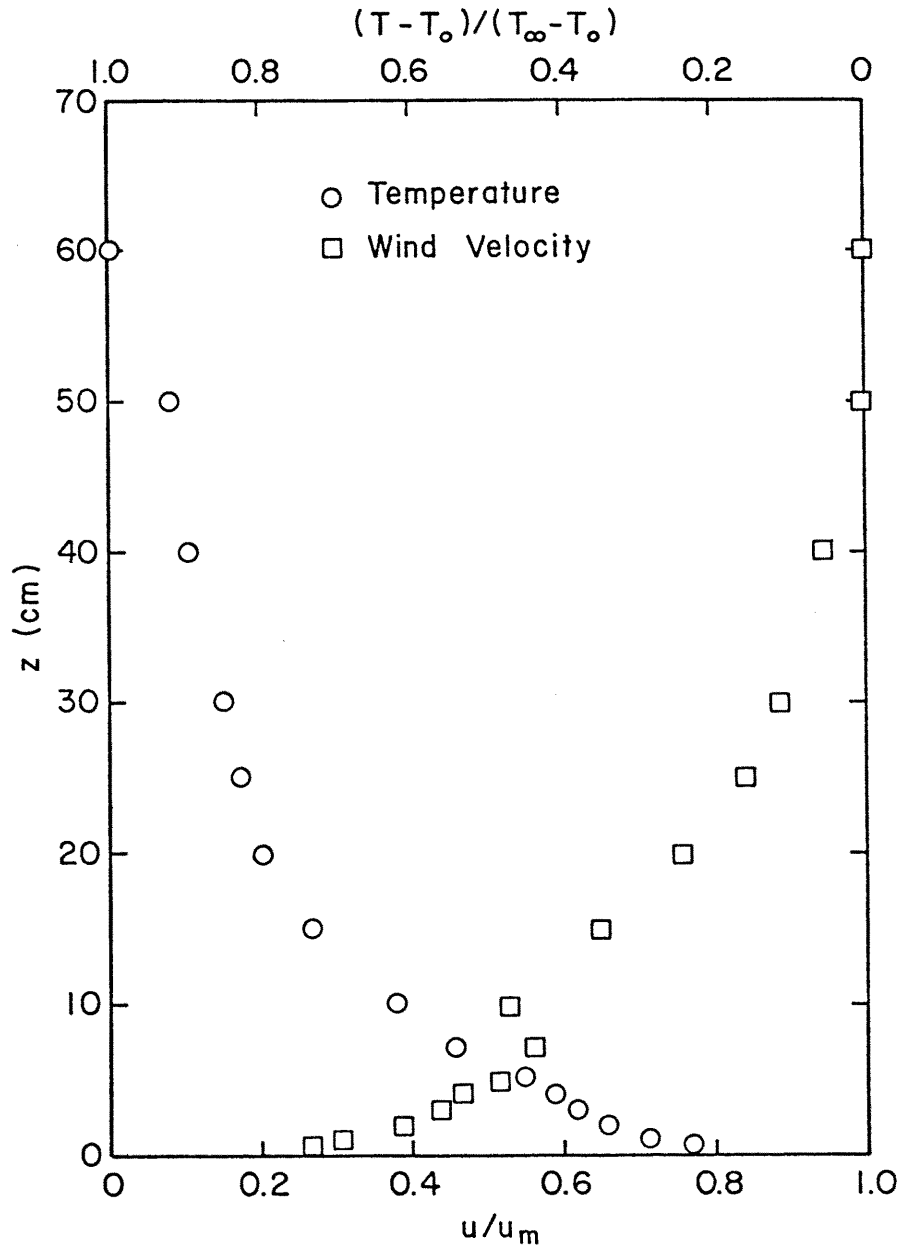


Figure 5-6. Dimensionless Velocity and Temperature Profile at Location No. 6 for $T_o = 4.5^\circ\text{C}$, $T_\infty = 56.1^\circ\text{C}$ and $u_m = 1.078$ m/sec.

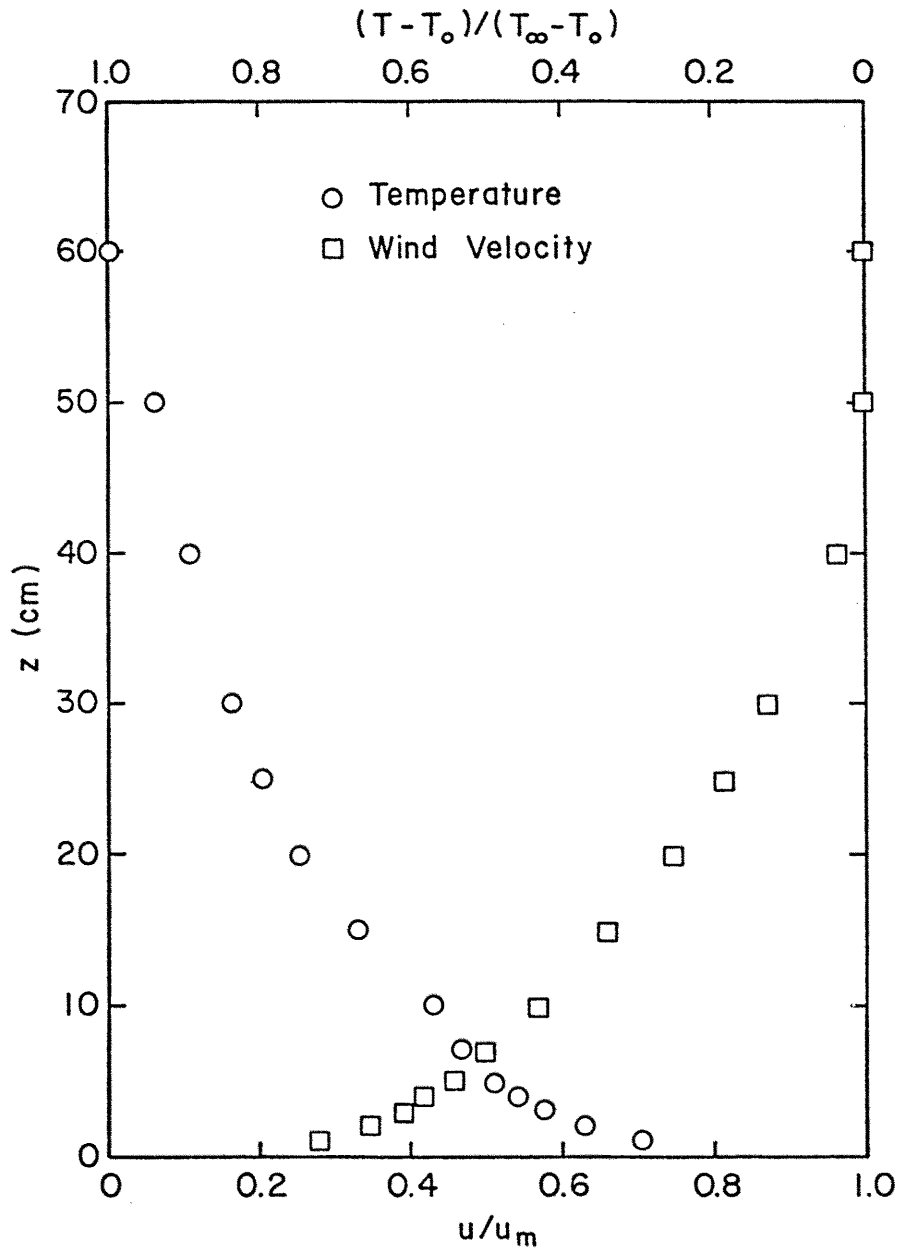
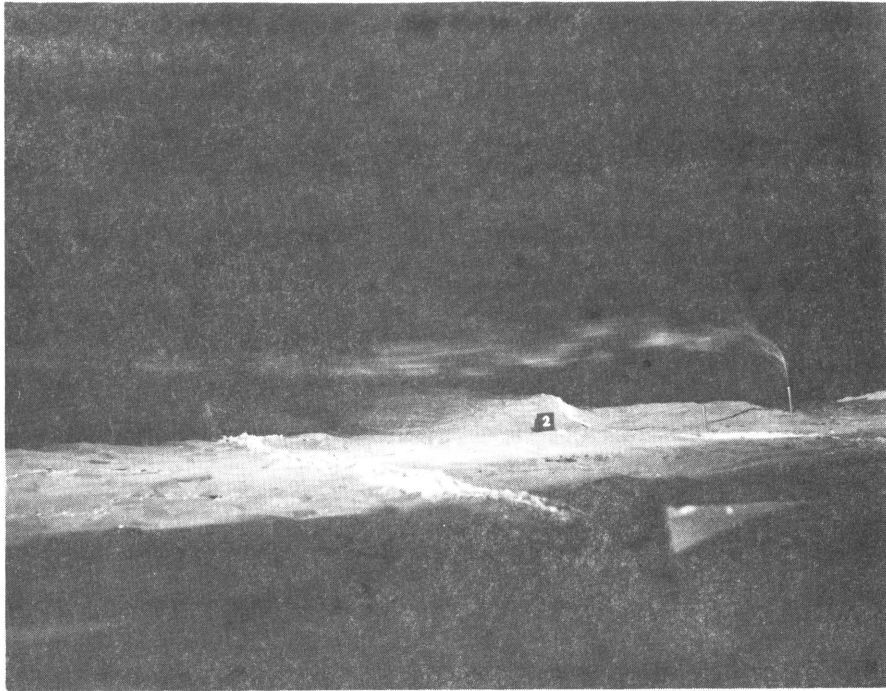


Figure 5-7. Dimensionless Velocity and Temperature Profile at Location No. 7 for $T_o = 6.1^\circ\text{C}$, $T_\infty = 56.8^\circ\text{C}$ and $u_m = 0.935$ m/sec.



a)



b)

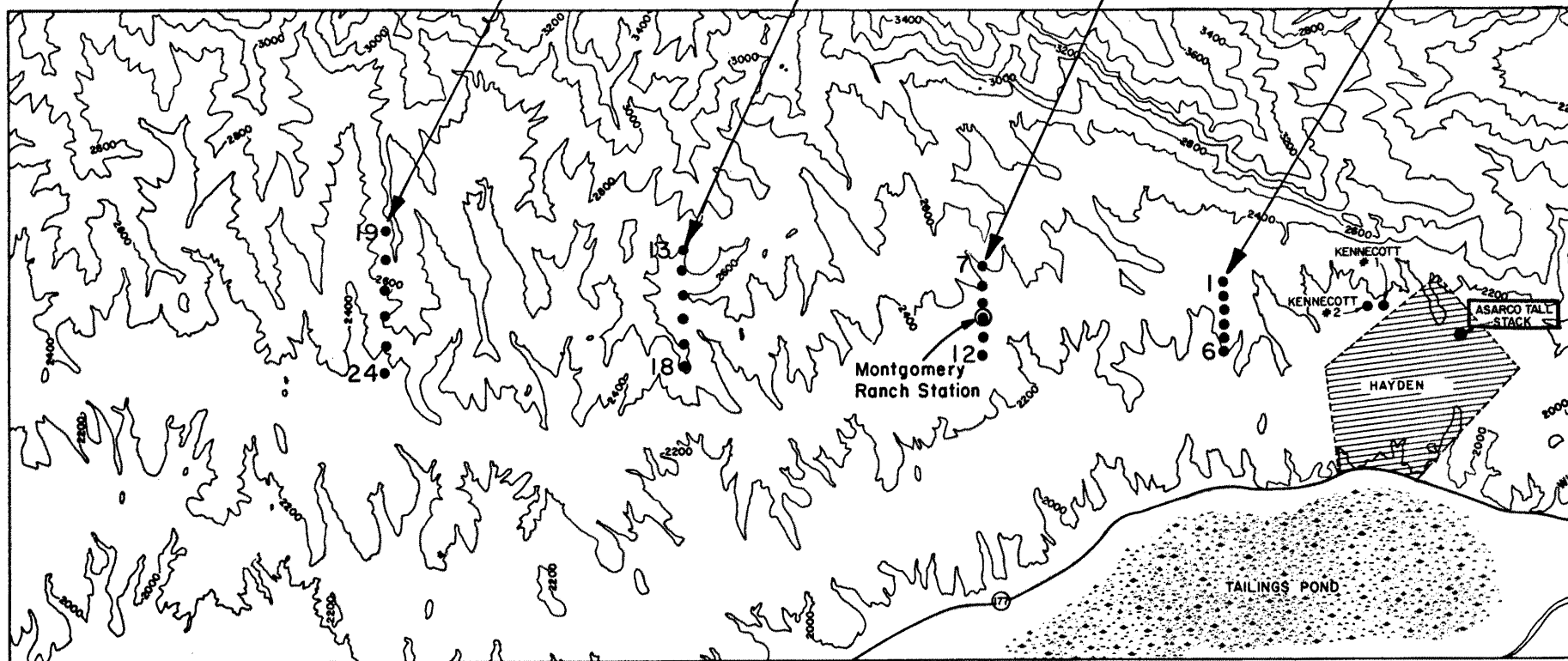
Figure 5-8. Photograph of Plume Transport from a) ASARCO Tall Stack and b) Kennecott Tall Stack under Stable Stratification for a Southeast Wind.

19	0
20	0.011
21	0.002
22	0.005
23	0.007
24	0.011

13	0.009
14	0.002
15	
16	0.009
17	0.015
18	0.005

7	0.011
8	0.013
9	0.016
10	0.022
11	0.027
12	0.002

1	0.004
2	0.015
3	0.016
4	0.018
5	0.016
6	0.009



0.5 0 1 KILOMETER
SCALE

● Ground Level Concentration
Measurement Points

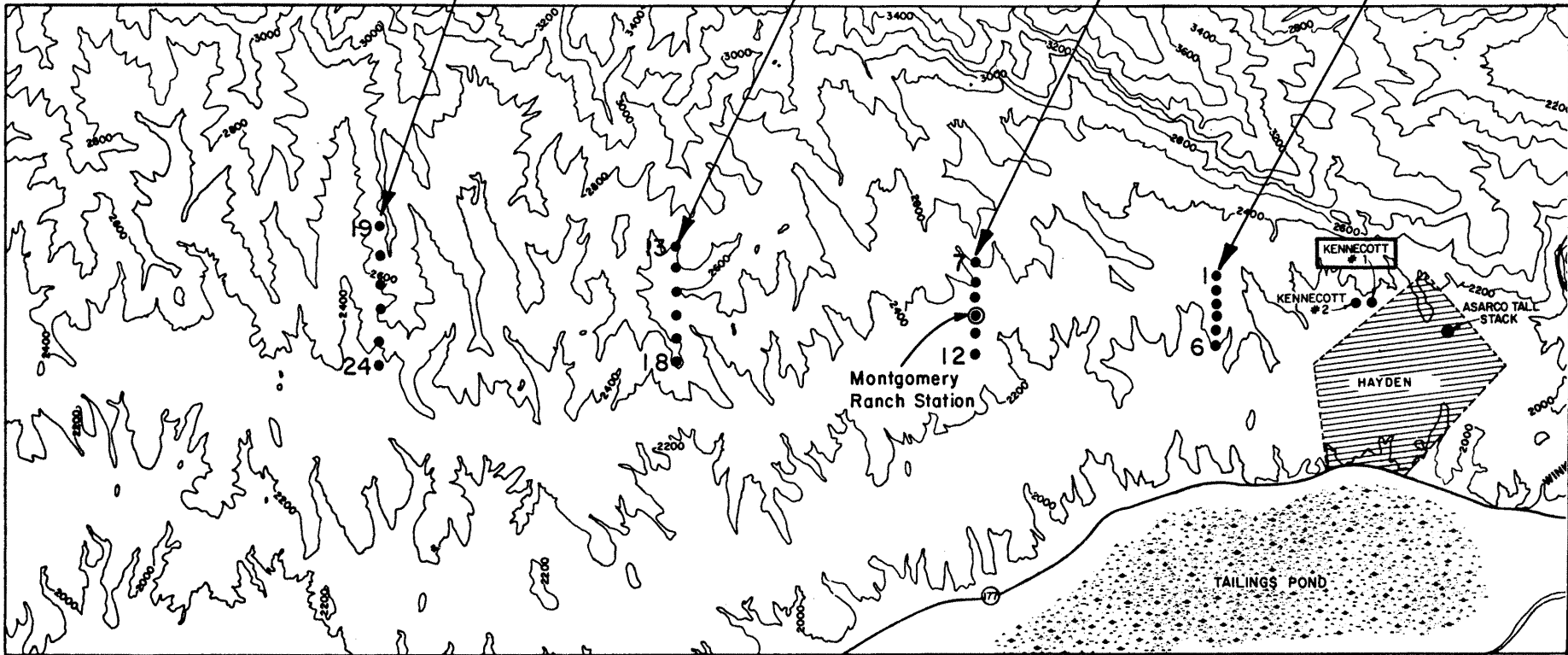
Figure 5-9. Results of Concentration Measurements for ASARCO Tall Stack. (The numbers in the box are location # and equivalent SO₂ concentration in ppm.)

19	
20	0.004
21	0
22	0.004
23	0.005
24	0.005

13	0.005
14	0
15	
16	0.015
17	0.018
18	0.009

7	0.007
8	0.015
9	0.027
10	0.040
11	0.049
12	0.002

1	0.009
2	0.020
3	0.020
4	0.020
5	0.015
6	0.002



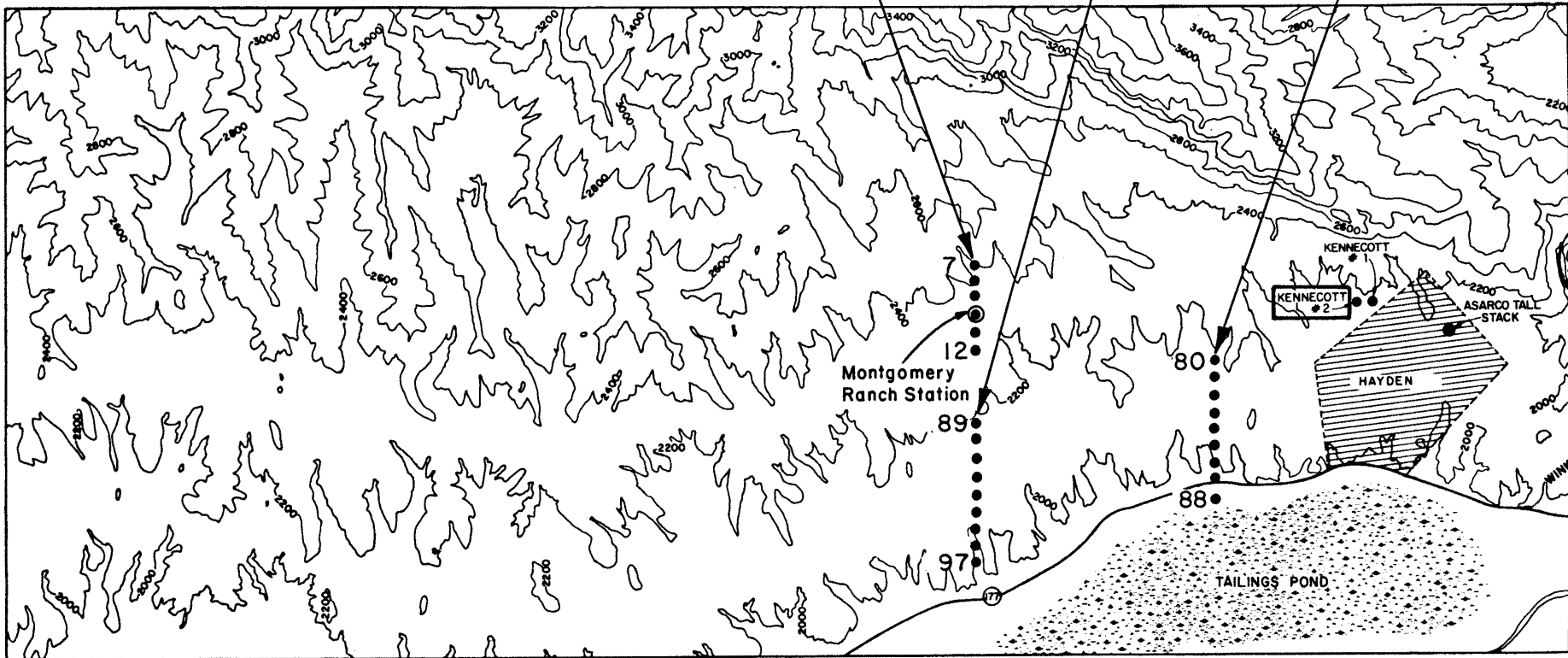
● Ground Level Concentration Measurement Points

Figure 5-10. Results of Concentration Measurements for Kennecott Tail Stack (Kennecott #1). (The numbers in the box are location # and equivalent SO₂ concentration in ppm.)

7	0.004
8	0.005
9	0.013
10	0.015
11	0.018
12	0.005

89	0.016
90	0.013
91	0.015
92	0.015
93	0.015
94	0.013
95	0.013
96	0.015
97	0.009

80	0.166
81	0.162
82	0.187
83	0.237
84	0.186
85	0.269
86	0.269
87	0.235
88	0.177



● Ground Level Concentration Measurement Points

Figure 5-11. Results of Concentration Measurements for Kennecott Short Stack (Kennecott #2). The Numbers in the Box are Location # and Equivalent SO₂ Concentration in ppm. (Results for 60 tons/day sulphur emission rate are as indicated except x 10.)

TABLES

Table 3.1. Model and Prototype Parameters for the ASARCO-Stable Evaluation.

PARAMETER:	Test Series:	ASARCO		KENNECOTT #1		KENNECOTT #2	
		PROTOTYPE	MODEL	PROTOTYPE	MODEL	PROTOTYPE	MODEL
1) Stack Height - H_s (m)		304.9	0.099	182.9	0.060	24.4	0.0079
2) Stack Diameter - D(m)		5.18	0.00506	4.7	0.00765	2.41	0.00141
3) Load (%)		100		100		100	
4) Free Stream Velocity - u_∞ (m/s)		10.0	0.78	10.0	0.78	10.0	0.78
5) Exit Velocity - u_s (m/s)		14.7	0.74	7.6	0.21	10.4	0.63
6) Volume Flow - V(m ³ /s)		310.8	1.488 E-05	132.2	9.652 E-06	47.2	9.837 E-07
7) Ambient Temperature - T(^o K)		293	306	293	306	293	306
8) Exit Temperature - T_s		388.6	306	476.3	306	316.3	306
9) Density Ratio - $\gamma \left(\frac{T_s - T_a}{T_s} \right)$ or $\left(\frac{\rho_a - \rho_s}{\rho_a} \right)$		0.25	0.80	0.38	0.80	0.07	0.523
10) Froude Number - $Fr = \frac{u_s}{\sqrt{g\gamma D}}$		4.126	3.70	1.82	0.86	8.09	7.40
11) Velocity Ratio - $R \left(\frac{u_s}{u_\infty} \right)$		1.47	0.95	0.76	0.27	1.04	0.81
12) Momentum Ratio - $M_o \left[(1-\gamma) R^2 D^2 / H_s^2 \right]$		0.00047	0.00047	0.00024	0.00024	0.0098	0.0098
13) Buoyancy Ratio - $B_o \left[\frac{R^3}{Fr^2} \frac{D}{H_s} \right]$		0.0032	0.0032	0.0034	0.0034	0.00170	0.00170
14) Emission Rate - Q_s (gm/s)		5591	--	1219	--	$\frac{126}{(1261)^1}$	--
15) Surface Temperature - T_o (^o K)		291.7	281				
16) Free Stream Temperature - T_∞ (^o K)		294.3	331				
17) Free Stream Height - δ (m)		600	0.20				
18) Bulk Richardson Number - Ri		0.53	0.53				
$Ri = \frac{g}{T} \frac{(T_\infty - T_o)\delta}{u_\infty^2}$							

¹Two emission rates for 6 and 60 tons/day sulphur as described in Appendix A, September 26, 1979 letter.

Table 5.1. Velocity and Temperature Profile at
Location 1. (See Figure 4-2) - $T_o = 6.5^{\circ}\text{C}$

z (m)	u (m/s)	$T - T_o$ ($^{\circ}\text{C}$)
.002	0.337	7.8
.004	0.409	7.3
.007	0.439	7.5
.010	0.475	8.5
.015	0.515	10.6
.020	0.546	13.6
.025	0.577	15.8
.030	0.599	18.2
.040	0.635	23.5
.050	0.650	27.8
.060	0.657	30.4
.080	0.671	33.1
.100	0.690	34.6
.130	0.726	36.2
.160	0.755	37.5
.200	0.813	40.3
.250	0.860	42.2
.300	0.913	44.4
.350	0.939	45.8
.400	0.964	47.0
.500	0.954	49.0
.600	0.904	50.7

Table 5.2. Velocity and Temperature Profile at
Location 2. (See Figure 4-2) - $T_o = 10.5^\circ\text{C}$

z (m)	u (m/s)	$T - T_o$ ($^\circ\text{C}$)
.002	0.222	10.4
.004	0.321	11.3
.007	0.349	12.2
.010	0.390	13.0
.015	0.425	15.3
.020	0.471	16.5
.025	0.489	18.8
.030	0.508	19.2
.040	0.494	20.2
.050	0.526	22.1
.060	0.565	23.1
.080	0.563	27.0
.100	0.601	30.3
.130	0.655	35.8
.160	0.698	38.0
.200	0.753	39.3
.250	0.794	40.7
.300	0.828	41.6
.350	0.848	42.0
.400	0.864	42.6
.500	0.886	45.3
.600	0.876	48.0
.639	0.866	49.7

Table 5.3. Velocity and Temperature Profile at
Location 3. (See Figure 4-2) - $T_o = 11.5^{\circ}\text{C}$

z (m)	u (m/s)	$T - T_o$ ($^{\circ}\text{C}$)
.002	0.203	16.4
.004	0.252	20.7
.007	0.293	22.5
.010	0.305	23.4
.015	0.348	24.5
.020	0.365	25.5
.025	0.403	26.7
.030	0.439	27.1
.040	0.514	27.9
.050	0.604	29.9
.060	0.681	31.8
.080	0.743	34.6
.100	0.764	36.2
.130	0.827	37.7
.160	0.848	38.7
.200	0.903	39.8
.250	0.955	40.9
.300	0.971	42.5
.350	0.972	44.1
.400	0.955	45.7
.500	0.895	46.9
.600	0.804	47.5

Table 5.4. Velocity and Temperature Profile at
Location 4. (See Figure 4-2) - $T_o = 9.1^{\circ}\text{C}$

z (m)	u (m/s)	$T - T_o$ ($^{\circ}\text{C}$)
.004	0.181	13.6
.007	0.205	15.9
.010	0.213	16.6
.015	0.229	17.3
.020	0.265	19.4
.025	0.280	20.6
.030	0.299	22.0
.040	0.374	23.2
.050	0.437	26.3
.070	0.519	29.2
.100	0.610	32.6
.150	0.731	36.0
.200	0.828	38.1
.250	0.921	39.9
.300	0.981	41.1
.400	1.070	43.8
.500	1.106	46.8
.600	1.039	48.3

Table 5.5. Velocity and Temperature Profile at
Location 5. (See Figure 4-2) - $T_o = 8.2^{\circ}\text{C}$

z (m)	u (m/s)	$T - T_o$ ($^{\circ}\text{C}$)
.004	0.349	15.2
.007	0.382	18.7
.010	0.389	19.5
.015	0.408	20.4
.020	0.427	21.8
.025	0.453	22.3
.030	0.486	23.5
.040	0.504	24.7
.050	0.538	26.0
.070	0.635	28.7
.100	0.705	31.6
.150	0.759	35.1
.200	0.803	37.0
.250	0.859	39.1
.300	0.953	41.8
.400	1.064	44.3
.500	1.087	45.9
.590	1.086	48.6

Table 5.6. Velocity and Temperature Profile at
Location 6. (See Figure 4-2) - $T_o = 4.5^\circ\text{C}$

z (m)	u (m/s)	$T - T_o$ ($^\circ\text{C}$)
.004	0.290	11.6
.007	0.316	13.1
.010	0.334	14.8
.015	0.375	16.0
.020	0.422	17.7
.025	0.429	18.8
.030	0.473	19.7
.040	0.504	21.2
.050	0.558	23.1
.070	0.609	27.8
.100	0.569	32.0
.150	0.703	37.7
.200	0.819	41.0
.250	0.908	42.7
.300	0.958	43.8
.400	1.029	46.1
.500	1.074	47.5
.600	1.078	51.6

Table 5.7. Velocity and Temperature Profile at Location 7. (See Figure 4-2) - $T_o = 6.1^{\circ}\text{C}$

z (m)	u (m/s)	$T - T_o$ ($^{\circ}\text{C}$)
.007	0.218	13.6
.010	0.261	14.9
.015	0.289	16.7
.020	0.322	18.6
.025	0.334	20.0
.030	0.365	21.4
.040	0.391	23.0
.050	0.428	24.8
.070	0.468	26.9
.100	0.528	28.9
.150	0.614	33.9
.200	0.695	37.8
.250	0.761	40.3
.300	0.817	42.4
.400	0.901	45.3
.500	0.935	47.6
.600	0.930	50.7

Table 5.8. Example of Power Law Exponent Variations with Stability from a) Touma, 1977 and b) Sutton, 1953

a) Touma, 1977

Stability Class	Missouri ^a 1973-74	Missouri ^a 1974-75	Kansas ^a 1973-74	Kansas ^a 1974-75	Iowa ^a 1973-74	Texas ^a 1973-74	Michigan ^a 1975-76	Missouri ^b 1973-74
A	0.103	0.099	0.124	0.091	0.104	0.120	0.109	0.111
B	0.079	0.092	0.145	0.103	0.101	0.123	0.085	0.119
C	0.082	0.080	0.152	0.122	0.114	0.128	0.078	0.104
D	0.115	0.144 ^c	0.199	0.172	0.188	0.174	0.116	0.136
E	0.271	0.273	0.341	0.282	0.313	0.331	0.261	0.272
F	0.423	0.385	0.480	0.412	0.466	0.562	0.425	0.242
G	0.504	0.417	0.506	0.452	0.444	0.624	0.516	0.447
Terrain	Rolling	Rolling	Rolling	Rolling	Rolling	Rolling	Hilly	Rolling

^aStability class based on a ΔT of 10 to 60 m.

^bStability class based on a ΔT of 10 to 90 m.

b) Sutton, 1953

$\Delta T = T_{400'} - T_{5'} (^{\circ}\text{F})$	n
0 to 2	0.32
2 to 4	0.44
4 to 6	0.59
6 to 8	0.63
8 to 10	0.62
10 to 12	0.77

Table 5.9. Summary of Velocity Profile Characteristics

No.	u^* (cm/s)	z_o (cm)	$1/L$ (m^{-1})	$Re_{z_o}^*$	n	$e_{z_o}^{1)}$	$e_n^{2)}$
1	5.52	0.013	0.16	0.48	0.18	0.039	0.035
2	5.65	0.035	0.19	1.32	0.22	0.038	0.036
3	11.19	0.232	-0.55	17.31	0.30	0.103	0.128
4	10.42	0.460	0.21	31.95	0.42	0.100	0.073
5	6.17	0.051	0.80	2.10	0.25	0.051	0.043
6	6.88	0.095	0.64	4.35	0.28	0.055	0.043
7	6.81	0.201	0.55	9.13	0.34	0.038	0.026

* $\nu = 0.15 \text{ cm}^2/\text{s}$

1) The root-mean-square error (m/s) between log-law and observation.

2) The root-mean-square error (m/s) between power-law and observation.

Table 5.10. Concentration Results for ASARCO Tall Stack

Location	Description:	SO ₂ Concentration (ppb)		AVERAGE
		REPEAT 1	REPEAT 2	
1		2	4	3
2		9	20	15
3		9	22	16
4		11	24	18
5		11	20	16
6		7	9	8
7		11	-	11
8		11	15	13
9		15	18	16
10		16	27	22
11		18	35	27
12		2	0	2
13		7	9	8
14		2	-	2
15		-	-	-
16		7	11	9
17		13	16	15
18		5	4	5
19		-	-	-
20		-	11	11
21		2	2	2
22		5	-	5
23		7	-	7
24		11	9	11
25		-	-	-

Table 5.11. Concentration Results for Kennecott Stack #1

Location	Description:	SO ₂ Concentration (ppb)		AVERAGE
		REPEAT 1	REPEAT 2	
1		-	9	9
2		11	27	19
3		11	27	19
4		11	27	19
5		7	22	15
6		-	2	2
7		2	11	7
8		9	20	15
9		18	35	27
10		31	47	39
11		40	56	48
12		-	2	2
13		-	5	5
14		-	-	-
15		-	-	-
16		9	18	14
17		13	22	18
18		-	9	9
19		-	-	-
20		-	4	4
21		-	-	-
22		-	4	4
23		-	5	5
24		2	9	6

Table 5.12. Concentration Results for Kennecott Stack #2
(6 tons/day sulphur emission rate¹)

Location	Description:	SO ₂ Concentration		AVERAGE
		REPEAT 1	REPEAT 2	
1		-	-	-
2		-	-	-
3		-	-	-
4		-	-	-
5		-	-	-
6		-	-	-
7		4	-	4
8		5	5	5
9		7	16	12
10		15	-	15
11		18	16	17
12		5	-	5
80		160	171	166
81		158	166	162
82		191	184	187
83		248	224	236
84		195	175	185
85		268	269	268
86		268	269	268
87		237	233	235
88		177	-	177
89		16	15	16
90		15	9	12
91		15	13	14
92		16	13	15
93		7	4	5
94		15	11	13
95		15	11	13
96		15	13	14
97		11	7	9

¹for 60 tons/day multiply results x 10

Table 5.13. Summary of Stable Wind Tunnel Tests for ASARCO

POINT NO: STACK:	SO ₂ CONCENTRATION								EMISSION RATE									
	No. 7		No. 8		No. 9		No. 10		No. 11		No. 12		AVERAGE		g/s		%	
	ppm	%	ppm	%	ppm	%	ppm	%	ppm	%	ppm	%	ppm	%				
ASARCO	0.011	50	0.013	39	0.016	29	0.022	29	0.027	29	0.002	20	0.015	30	5591	80		
KENNECOTT #1	0.007	33	0.015	44	0.027	48	0.040	52	0.049	52	0.002	20	0.023	48	1219	18		
KENNECOTT #2 (6 tons/day)	0.004	17	0.006	17	0.013	23	0.015	19	0.018	19	0.006	60	0.011	22	126	2		
(60 tons/day)	(0.036)		(0.055)		(0.127)		(0.146)		(0.182)		(0.055)		(0.109)		(1261)			
TOTAL (TOTAL)	0.022	100	0.034	100	0.053	100	0.077	100	0.094	100	0.010	100	0.049	100	6956	100		
	(0.054)		(0.083)		(0.170)		(0.208)		(0.258)		(0.059)		(0.147)		(8071)			

APPENDIX A

Project Correspondence

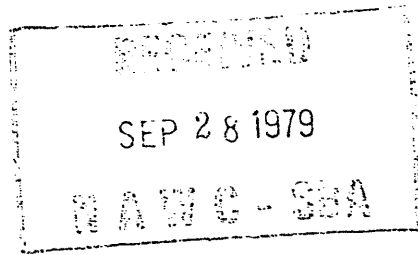
ASARCO

Hayden Plant

Lary G. Cahill
Manager

David J. Parker
General Superintendent

Robert A. Moon
Accounting Manager



September 26, 1979

Mr. George Taylor
North American Weather Consultants
600 Norman Firestone Road
Santa Barbara Municipal Airport
Goleta, CA 93017

Dear Mr. Taylor:

This letter confirms Asarco's desire to have additional wind tunnel fluid model studies performed under stable nighttime conditions with a wind direction of 125° to 130°.

This will be a three-stack release using the following information:

<u>Parameter</u>	<u>Asarco</u>	<u>Kennecott</u>	<u>Kennecott</u>
Stack Height (Ft.)	1,000	600	80
Base Elevation (Ft. MSL)	2,184	2,204	2,205
Exit Temp. (°F)	240	398	110
Volume (Cfm)	658,000	280,000	100,000
Exit Diameter (Ft.)	17	15.4	7.9
Sulfur (Tons/Day)	266	58	6

The given sulfur output for the Kennecott 80-foot acid plant stack is for optimum operating conditions. Recently, for a three-hour period, the hourly sulfur output from this facility was 60 tons/day. Shortly after this time period, the ambient air standards were exceeded at the Montgomery Ranch station. Therefore, it would be desirable to model both the 6 tons/day and 60 tons/day emission rates from this facility.

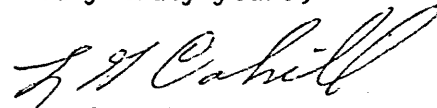
Mr. George Taylor

-2-

September 26, 1979

The cost estimate of \$27,750 submitted by North American Weather Consultants on May 9, 1979, may not be exceeded without approval by Asarco.

Very truly yours,



L. G. Cahill

LGC:cch

cc: L. C. Travis
K. W. Nelson
J. L. Woods
N. R. Porter
C. K. Guptill

**NORTH AMERICAN WEATHER CONSULTANTS**

TELEPHONE (805) 967-1246

600 NORMAN FIRESTONE ROAD ■ GOLETA, CA 93017

December 10, 1979

Dr. Ronald L. Petersen
Fluid Dynamics and Diffusion Laboratory
Colorado State University
Fort Collins, CO

Dear Dr. Petersen:

At the request of ASARCO Incorporated, North American Weather Consultants (NAWC) wishes to confirm our earlier verbal agreement to conduct wind tunnel modeling under stable nighttime conditions in the Hayden, Arizona area. I am enclosing a copy of a letter from ASARCO listing the relevant stack parameters for the emission sources to be modeled.

In our earlier conversations, you indicated that total costs of the study would be approximately \$20,000. Please send me written confirmation of this figure, including itemized unit costs.

I look forward to working with you again. Please call me if you have any questions.

Very truly yours,

A handwritten signature in cursive script that reads 'George H. Taylor'.

George H. Taylor
Manager, Air Quality Field Studies

GHT:dmz/91

Enclosure

cc: Keith Brown
Einar Hovind